CONTRACTOR REPORT ARSCD-CR-78009

THERMAL ANALYSIS OF FOLDED AMMUNITION

EDWARD V. MC ASSEY, JR.
CHRISTINE M. EASTBURN

JANUARY 1979

US ARMY ARMAMENT RESEARCH AND DEVELOPMENT COMMAND
SMALL CALIBER
WEAPON SYSTEMS LABORATORY
DOVER, NEW JERSEY

APPROVED FOR PUBLIC RELEASE DISTRIBUTION UNLIMITED.

UNCLASSIFIED

SECURITY CLASSIFICATION OF THIS PAGE (When Data Entered)

REPORT DOCUMENTATION PAGE

READ INSTRUCTIONS BEFORE COMPLETING FORM

1. REPORT NUMBER Contractor Report ARSCD-CR-78009	2. GOVT ACCESSION NO.
3. RECIPIENT'S CATALOG NUMBER 9	
4. TITLE (and Subtitle) 6 Thermal Analysis of Folded Ammunition	5. TYPE OF REPORT & PERIOD COVERED Final rept. 1 Sep[redacted]77 - 30 Jun [redacted]78
	6. PERFORMING ORG. REPORT NUMBER
7. AUTHOR(s) 10 Edward V. McAssey, Jr — Villanova Univ. Christine M. Eastburn — ARRADCOM	8. CONTRACT OR GRANT NUMBER(s) 15 DAAK 10-77-M-2704
9. PERFORMING ORGANIZATION NAME AND ADDRESS Villanova University Dept. of Mech. Engineering Villanova, PA 19085	10. PROGRAM ELEMENT, PROJECT, TASK AREA & WORK UNIT NUMBERS 12 52p.
11. CONTROLLING OFFICE NAME AND ADDRESS Commander U.S. Army ARRADCOM, DRDAR-TSS Dover, NJ 07801	12. REPORT DATE 11 Jan[redacted]79
	13. NUMBER OF PAGES 46
14. MONITORING AGENCY NAME & ADDRESS (if different from Controlling Office) Commander U.S. Army ARRADCOM, FC&SCWSL Dover, NJ 07801	15. SECURITY CLASS. (of this report) Unclassified
	15a. DECLASSIFICATION/DOWNGRADING SCHEDULE

16. DISTRIBUTION STATEMENT (of this Report)

Approved for public release, distribution unlimited.

17. DISTRIBUTION STATEMENT (of the abstract entered in Block 20, if different from Report)

18 ARSCD, SBIE

19 CR-78009,
AD-E400 281

18. SUPPLEMENTARY NOTES

19. KEY WORDS (Continue on reverse side if necessary and identify by block number)

Heat Transfer
Folded Ammunition
Interior Ballistics
Ignition and Combustion
Single Base Propellant
Fluid Mechanics

20. ABSTRACT (Continue on reverse side if necessary and identify by block number)

The thermal response of the folded geometry cartridge has been determined. The heat input was determined for a 100 msec cycle. Temperature calculations were obtained for multiple firings of up to 29 rounds. The results indicated a peak surface temperature of approximately 1400°F after 600 rounds. This condition is considered to be no worse than would exist in conventional ammunition. However, the interface temperature between the cartridge case and the weapon will be more severe in the region near the base of the internose region. The magnitude of these temperatures will require further investigation.

DD FORM 1 JAN 73 1473 EDITION OF 1 NOV 65 IS OBSOLETE

Unclassified

SECURITY CLASSIFICATION OF THIS PAGE (When Data Entered)

409 253

REPRODUCED FROM BEST AVAILABLE COPY

JOB

TABLE OF CONTENTS

TABLES

FIGURES

INTRODUCTION

The objective of this investigation was to determine the temperature response of the "U-shaped" folded cartridge. Figure 1 presents a comparison of the conventional and folded cartridges. The interpose, or web region between the projectile and propellant reservoir, is of particular interest. Because of the unique geometry of the folded cartridge, this region of the weapon will experience heating on both sides, and the possibility of excessive temperatures or structural distortion exists.

To determine the temperature response of the interpose region, the heat input during a typical firing of 100 msec had to be established. In addition, analytical models describing the heat transfer of the folded cartridge geometry had to be developed. These models, one and two-dimensional, describe the transient temperature distribution using a finite difference technique. The models have been checked numerically to insure that nodal size provides an accurate representation. Since a time period longer than 100 msec is required for the weapon's structure to experience temperature change, the analytical model includes multiple firing bursts.

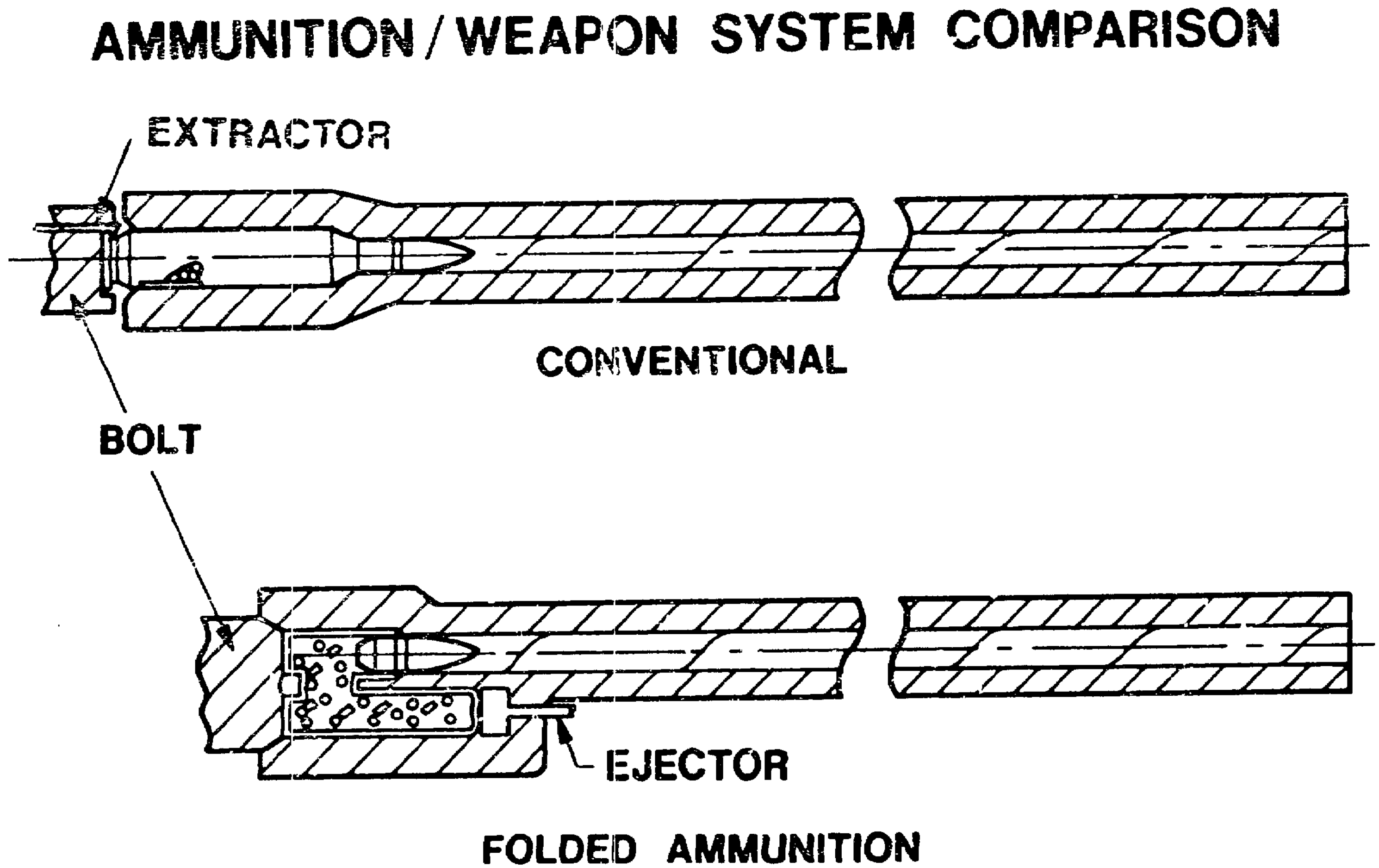

Figure 1. Geometry of folded ammunition.

HEATING ANALYSIS

The heat input cycle is 100 msec in duration. This period includes the firing of one cartridge, a dwell period, the extraction of the spent cartridge, and the insertion of a now cartridge. The highest heat fluxes occur during the firing time, or ballistic portion of the cycle. During this period the cartridge case is heated to its maximum temperature. Following this ballistic period, the energy deposited in the cartridge case dissipates into the weapon. To determine the heat transfer coefficient and gas temperature during the initial period, the local gas pressure, temperature, and velocity must be determined using the applicable ballistic model.

The ballistic model used in this study was supplied by U.S. ARRADCOM. This model, in the form of a computer code, is described in detail in reference 1. The code was developed for standard shape ammunition. The code, as supplied, has been modified to incorporate methods for determining thermochemical properties (ref. 2). Figure 2 presents the space mean pressure history for the folded cartridge calculated with the computer code.

As stated above, the model was not developed for ammunition of the present geometry; however, a review of reference 1 indicates that the model is insensitive to shape. The model does not provide for flame propagation through the propellant bed. Nonsimultaneous ignition is provided by the surface ignition function, which is equal to the total propellant surface area divided by the ignition time range. The latter quantity, ignition time range, is determined by experiment. Since the test case for the folded cartridge compares favorably with test firings, it appears that the ignition time range currently in the program is satisfactory. The three major pressures calculated by the program are the space mean pressure, the breech pressure, and the projectile base pressure. Both the breech and projectile base pressures are constant functions of the space mean pressure. All three pressures are made equal prior to movement of the projectile (approximately 0.34 msec for the present case).

The test case considers the breech to be 9.14 in. from the projectile. This corresponds to a straight cartridge 9.14 in. long from the base of the projectile to the end of the cartridge. A test case with the breech located 1.5 in. from the projectile was run. This corresponds to the folded geometry. The resulting pressures, temperatures, and muzzle velocities were not affected. It appears, therefore, that the only significant parameter is the propellant volume. The gas temperature and velocity are uniform over the entire region behind the projectile. This is significant because it indicates uniform heating.

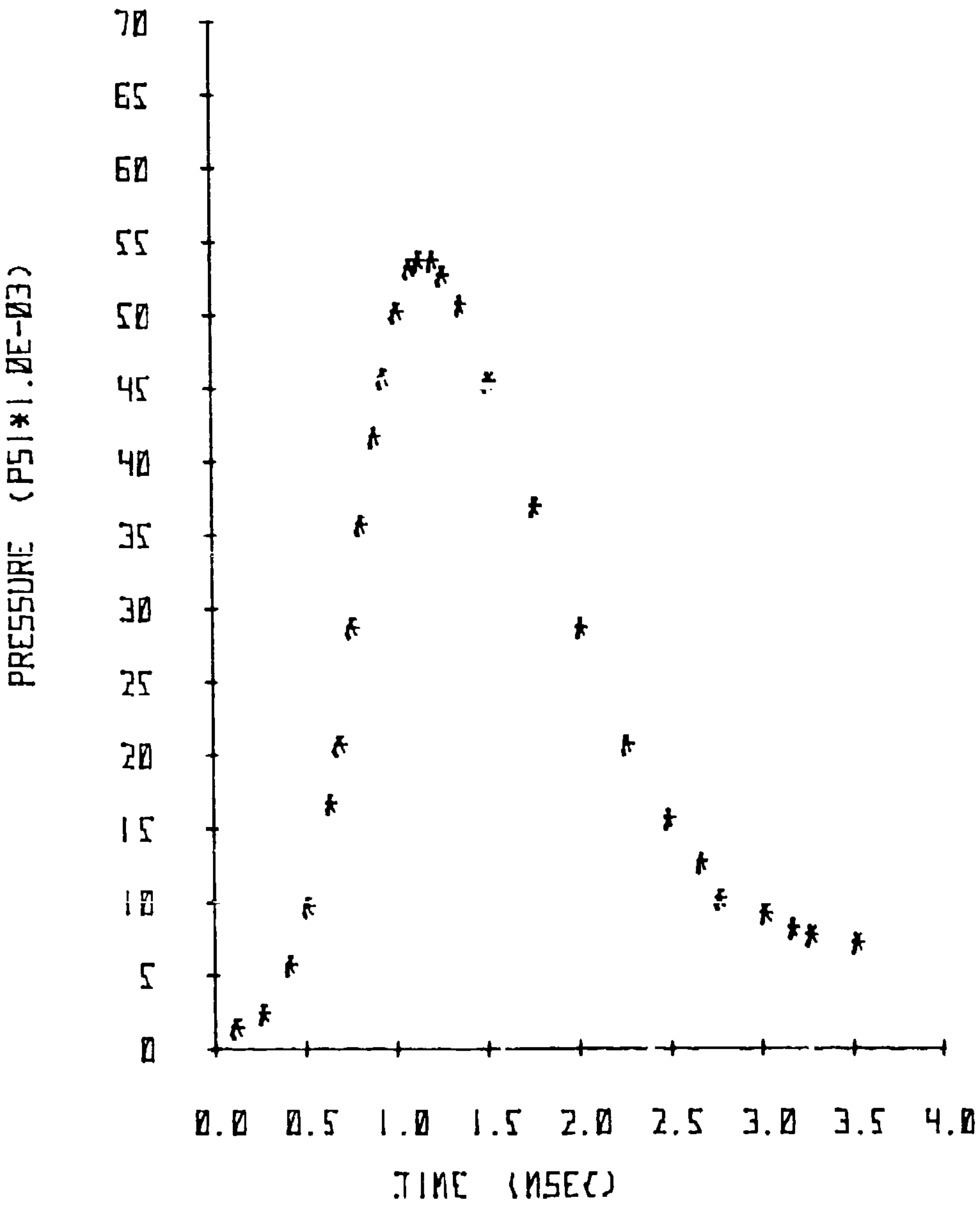

Figure 2. Space mean pressure versus time.

To accurately model nonuniform heating, a new ballistic model would have to be developed. This model would have to consider a one-dimensional transient flow allowing for finite flame propagation. This model could correctly position the initiation point and yield space dependent velocities, temperatures, and pressures. The decision regarding whether such a model should be developed will depend upon the need for improved ballistic data and the magnitude of the heating problem. However, the decision was made to use the existing model to establish the heating conditions in the folded geometry.

The flow conditions and temperature levels in the folded cartridge pose a severe heating environment for the cartridge case and surrounding weapon. Prediction of the heat transfer coefficient is also difficult because of the unique operating conditions.

Reference 3 provided heat transfer coefficients and temperature data for an environment similar to the present case. Unfortunately, the method used to make the calculations is not given. The maximum heat transfer coefficient is approximately 35×10^3 Btu/ft^{2}hr^{o}F. In addition, the maximum adiabatic wall temperature is 5700^oF. This is considerably higher than the value of 4065^oF obtained with the ballistic code, and it is also higher than the adiabatic flame temperature of the propellant.

Reference 4 was reviewed as a possible source of a heat transfer coefficient prediction method. This report examined a variety of possible prediction methods, but all required more flow field information than presently available. In addition, the report was more involved with the gun barrel, rather than the breech area. Some of the data presented indicated heat transfer coefficients in the range from 30×10^3 Btu/ft^{2}hr^{o}F to 70×10^3 Btu/ft^{2}hr^{o}F. It should be noted that these extreme levels exist for only 1 or 2 msec. Reference 5 evaluated the results of a method of characteristics study of the interior ballistics problem. The Colburn analogy, which is given by:

$$St\ P_r^{2/3} = C_f/2$$

where,

St = Stanton Number = Nu/Re Pr
Nu = Nusselt Number
Pr = Prandtl Number
Re = Reynolds Number
Cf = Friction factor

was used. The resulting heat transfer coefficients were in the same range as the previous references.

Reference 6 considered the problem of flow field development in a solid rocket motor. The operating conditions and dimensions were similar to the folded cartridge problem. This reference recommends

the Dittus Boelter correlation for local heat transfer coefficient. The Dittus Boelter equation is

$$Nu = 0.023\, Re^{.8}\, Pr^{.4}$$

The above equation is widely used in turbulent heat transfer calculations, and is relatively easy to apply to the present case. The decision was therefore made to use this relationship.

Assuming the gas to be ideal, and that the viscosity varies with the temperature to the 0.65 power, the heat transfer coefficient is given by:

$$h = 0.023 \left(\frac{PV}{R}\right)^{.8} C_P\, Pr^{-.6} \left(\frac{\mu_o}{D(530)^{.65}}\right)^{.2} T^{-.67}$$

where,

- P = pressure
- V = gas velocity
- Cp = specific heat
- μ_o = viscosity at 530° R
- D = diameter of chamber.

For the present case, the various constants are given by:

$$\mu_o = .87\times10^{-6}\, M^{.5}\,(530)^{.65} \qquad \text{(ref. 6)}$$

$$R = \frac{F}{T_o} = \frac{\text{propellant impetus}}{\text{flame temperature}} \qquad \text{(ref. 2)}$$

$$M = R_o/R$$

Using the thermochemical properties for the folded cartridge propellant and the ballistic data from the computer code, the heat transfer coefficients can be determined as a function of time. Figure 3 presents the variation of heat transfer coefficient versus time, based upon space mean pressure. Figure 4 presents the same data based upon projectile base pressure. For space mean pressure conditions, the peak heat transfer coefficient is approximately 52,500 Btu/ft^{2}hr^{o}F. This method for calculating heat transfer coefficient has been incorporated into the ballistic code. In addition, the stagnation temperature, which will be used in computing the convective heat inputs, has also been determined and is represented graphically in figure 5. It is worth noting that the maximum temperature in figure 5 is below that given in reference 3. This aspect of the results in reference 3 is difficult to explain. The peak temperatures reported in that reference are higher than the adiabatic flame temperature of the propellant used for the folded ammunition.

The heat transfer coefficients calculated with the Dittus Boelter equation are higher than those cited in reference 3, but are

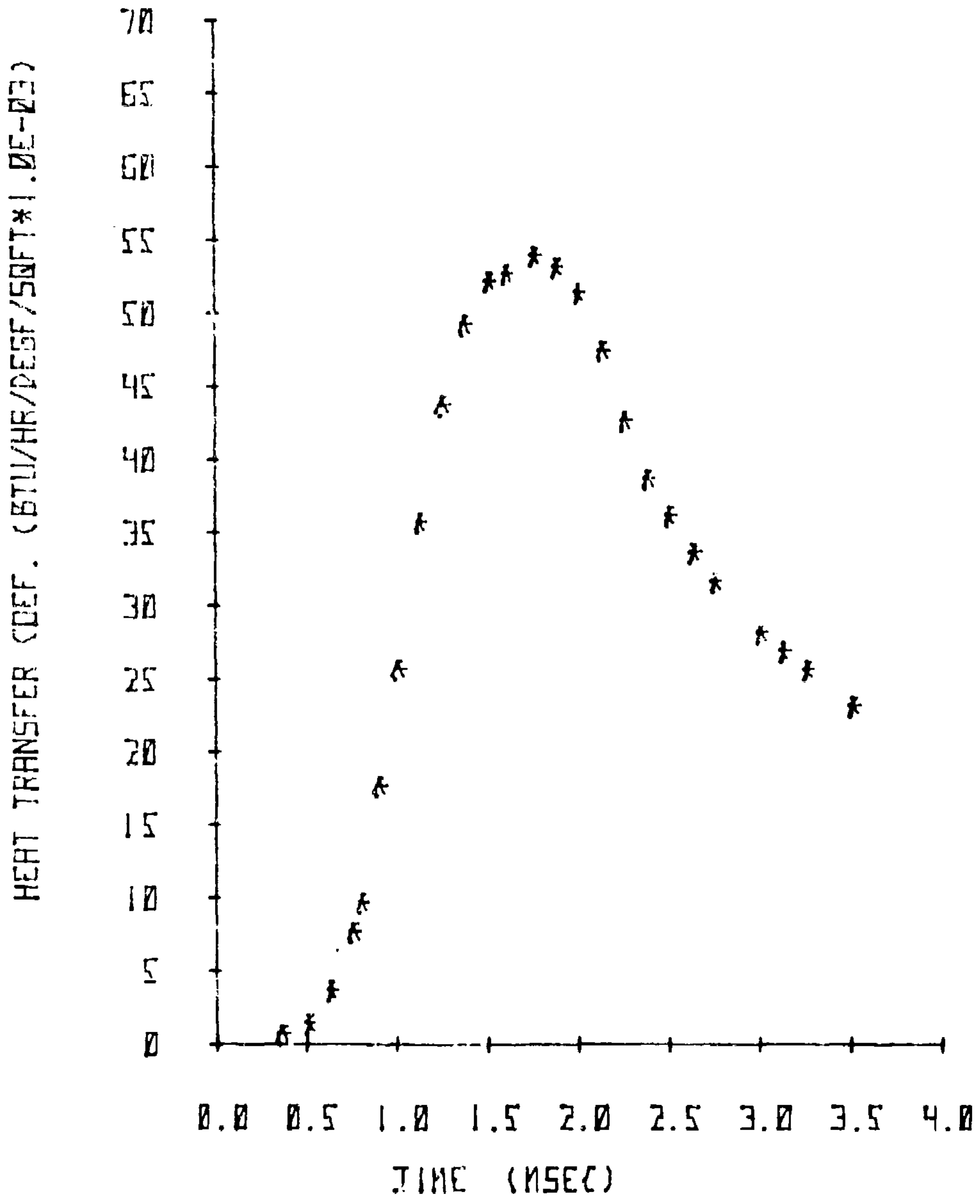

Figure 3. Heat transfer coefficient versus time - based upon space mean pressure.

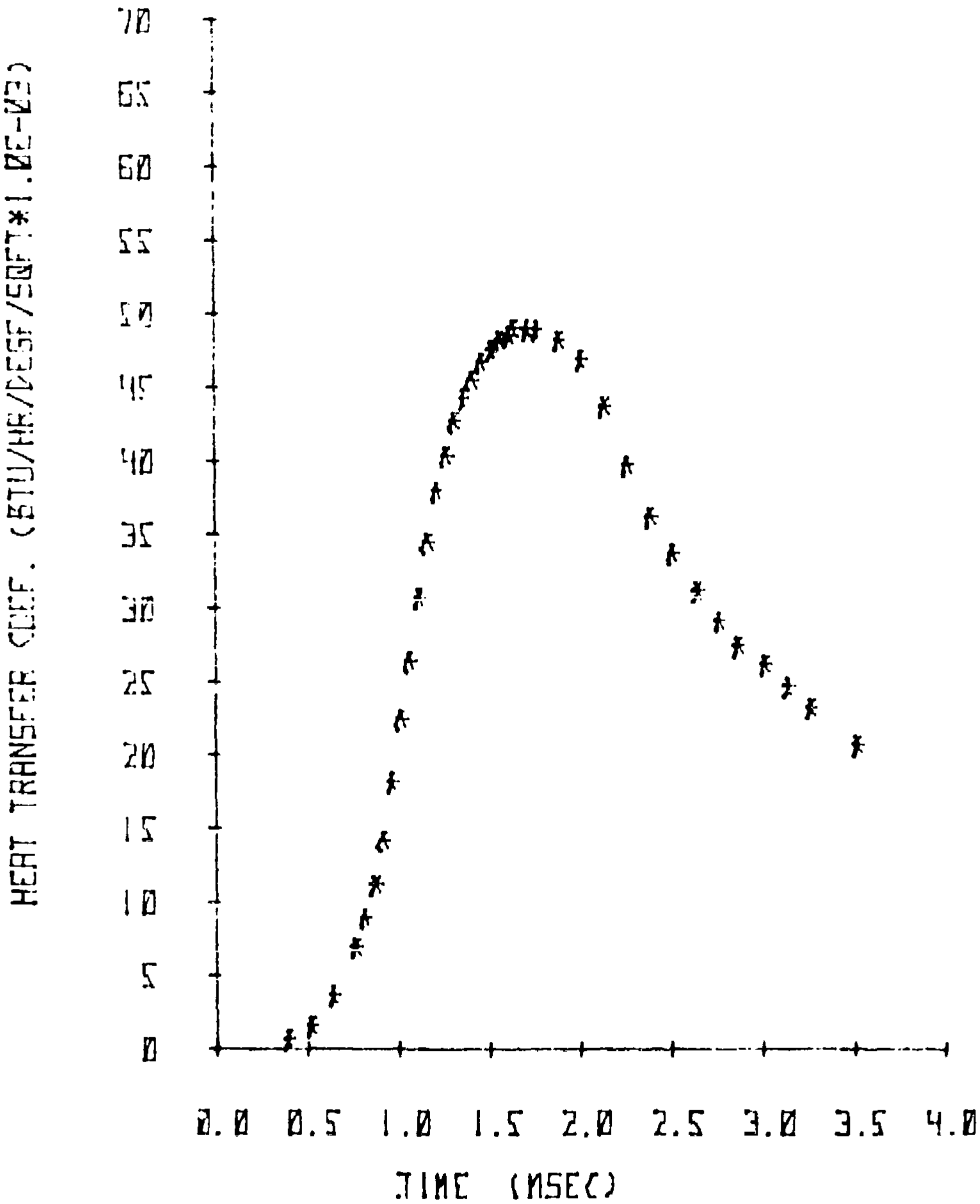

Figure 4. Heat transfer coefficient versus time - based upon projectile base pressure.

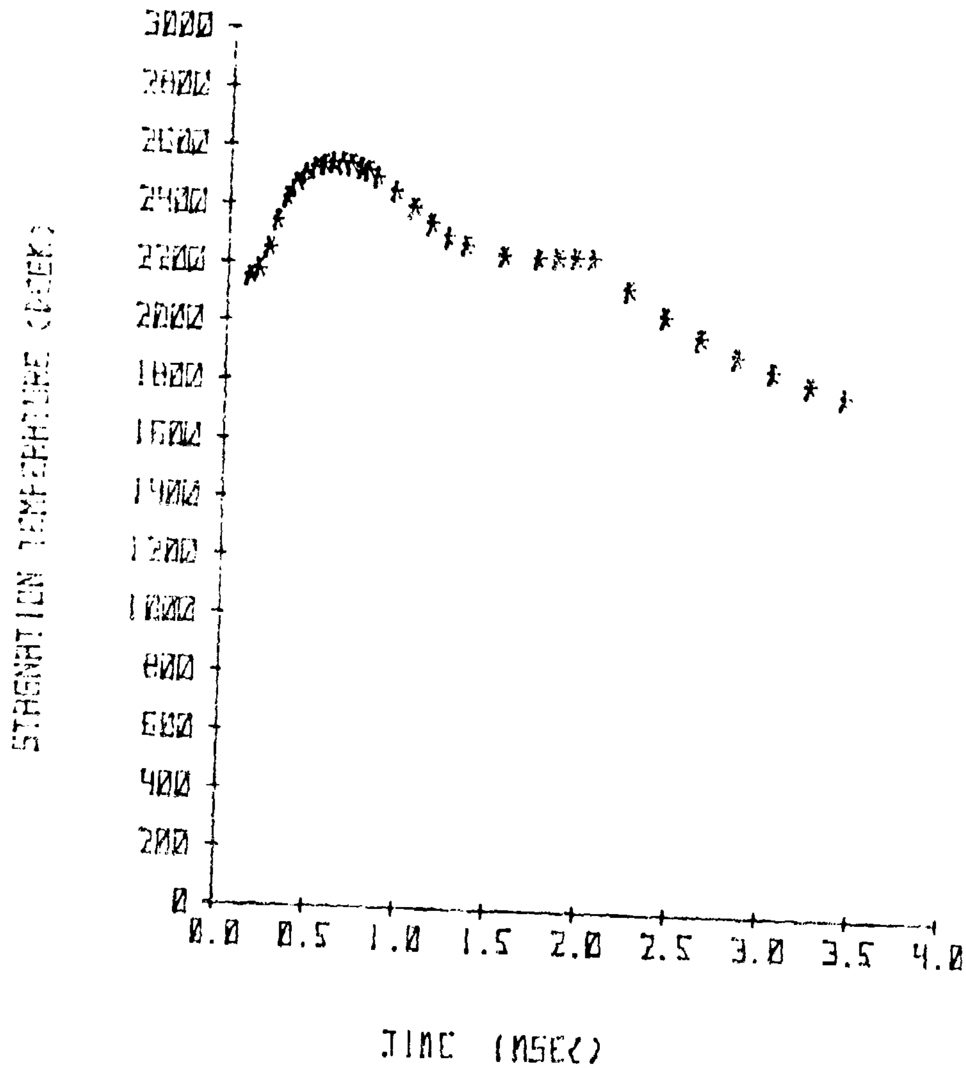

Figure 5. Stagnation temperature versus time.

well within the range reported by other references.

The heating conditions presented in figures 3 and 5 occur during the initial ballistic portion of the cycle, and last for approximately 3.5 msec. The peak surface temperature of the cartridge occurs during this portion of the cycle. However, the total time for the firing of a single cartridge is approximately 100 msec. It is during this longer period that the heat permeates into the weapon's structure and causes the highest structural temperatures.

The time history of a firing cycle is composed of the following four periods:

Time	Event
0 to 3.5 msec	Firing of projectile (ballistic portion)
3.5 to 35 msec	Dwell time
35 to 65 msec	Extraction of expended cartridge
65 to 100 msec	Loading of unspent cartridge

For the preceding firing cycle, the following heat inputs have been developed:

Time	Heat Inputs
0 to 3.5 msec	Convective heat input based upon Dittus Boelter equation (ref. 1). Figures 3 and 5 present the heat transfer coefficient and gas temperature profile.
3.5 to 35 msec	Exponential decay of the heat transfer coefficient to 100 Btu/ft^{2}hr$^\circ$F and of the gas temperature to 200°F.
35 to 65 msec	Constant heat transfer coefficient and gas temperature at 100 Btu/ft^{2}hr$^\circ$F and 200°F, respectively.
65 to 100 msec	Zero external heating. In addition, the cartridge nodes are returned to 100°F at 65 msec and then allowed to heat up due to the heat flow from the structure.

During the dwell time (3.5 to 35 msec), exponential decay of the gas pressure, gas temperature, and gas velocity is felt to be a reasonable approximation following the pressure decay. The value of 100 Btu/ft^{2}hr$^\circ$F for the heat transfer coefficient at 35 msec is conservative. The form of the heating boundary condition, during extraction and loading, is very difficult to describe. During future studies, experimental data would be examined to provide better insight into the thermal conditions during these phases of the operating cycle. For the present effort, the decision was made to use a conservative

approach and combine extraction and loading into a single instantaneous event at 65 msec. At 65 msec, the heat transfer coefficient was set at zero, and the nodes representing the cartridge case were set to 100°F. This simulates the chambering of an unspent cartridge. During the period from 65 to 100 msec, the cartridge case is cooler than the structure, and the heat flows into the cartridge.

Although the heat input profile used for this study is considered to be conservative, it should be examined further to determine the significance of the various assumptions made. This activity would be an interesting area for further effort.

ANALYTICAL MODELS

The detailed geometry of the folded cartridge case is given in figure 6. Since the heating during firing is uniform, based upon the present model, the problem reduces to the determination of two-dimensional temperature distributions. However, the results presented in reference 3 indicate that the depth of penetration of heat was small; therefore, the heat flow was essentially one-dimensional. Initial studies during this investigation verify this result. The majority of the results presented in the report will therefore be based upon one-dimensional models. However, in the web region near the breech, the geometry causes two-dimensional effects to occur. Two-dimensional results were obtained for this region.

One-Dimensional Model

The one-dimensional model consists of a 0.04 in. cartridge case thickness, and 0.50 in. of steel, which represents the weapon structure. The properties of the case material, cartridge brass and steel (SAE 4340), were obtained from reference 3. The temperatures were determined by dividing the model into a number of isothermal nodes, and solving the following equation using a digital computer:

$$T_i^{t+\Delta t} = \frac{\Delta t}{m_i c_i}\left\{\sum_j k_{ij} T_j^t + h A_i T_\infty\right\} + \left\{1 - \frac{\Delta t}{m_i c_i}\left(\sum_j k_{ij} + h A_i\right)\right\} T_i^t$$

where,

- k_{ij} = the conductive coupling between nodes
- $T_i^{t+\Delta t}$ = temperature of the i^{th} body at time $t + \Delta t$
- A_i = surface area of nodes exposed to convective (zero for all but surface node) heat transfer
- h = convective heat transfer coefficient
- T_∞ = gas temperature.

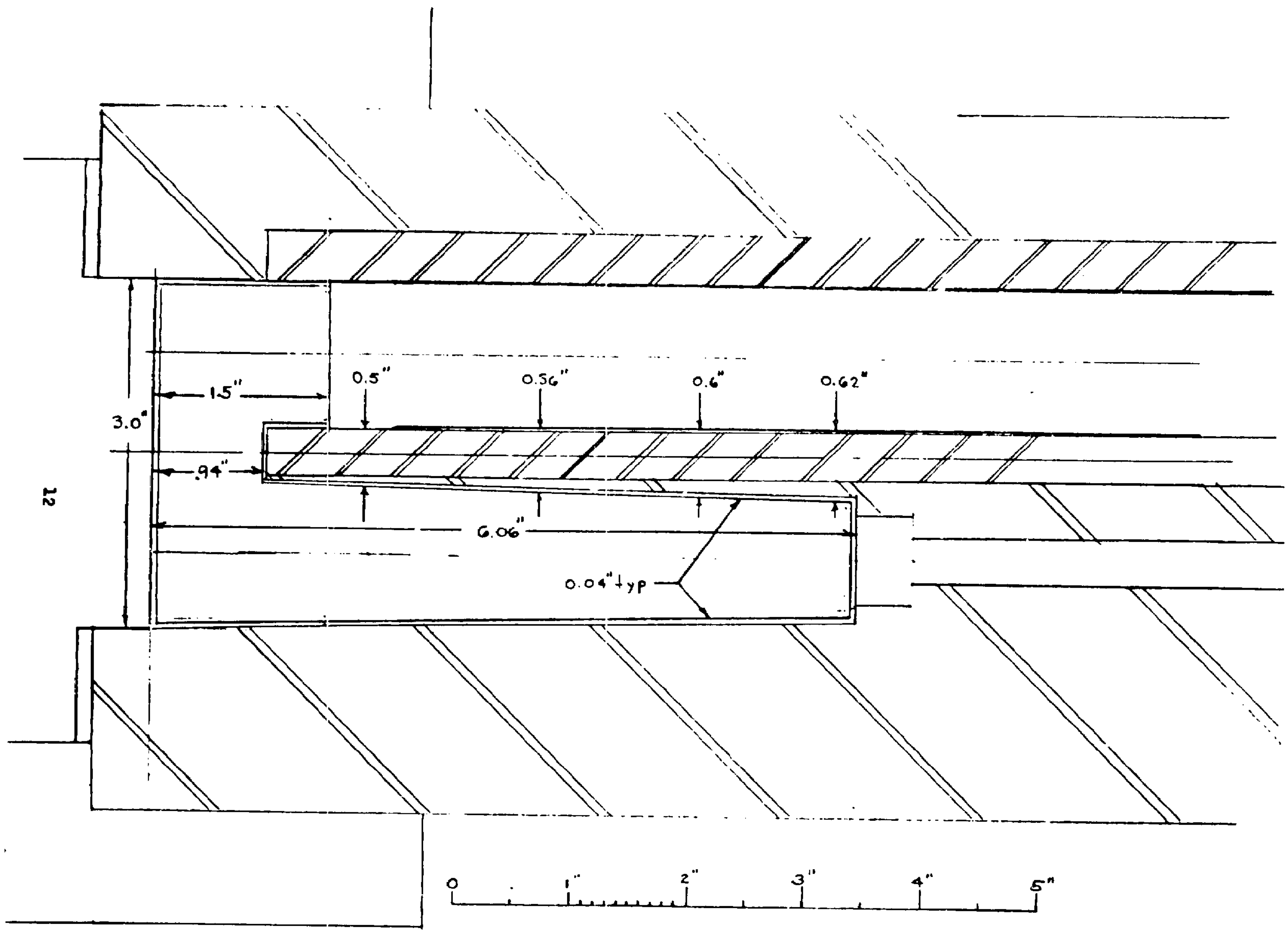

Figure 6. Detailed geometry of folded cartridge case.

Appendix A presents a listing of the computer program. In this analysis, both the heat transfer coefficient and the gas temperature are functions of time, as described in the Heating Analysis section of this report.

Two grid systems were initially used in the analysis. These are presented in table 1. The first system contains 26 bodies, with 11 bodies in the cartridge case, while the second contains 31 bodies, with 21 in the cartridge case. The use of more bodies in the cartridge case was initially felt to be necessary because of the rapid temperature changes occurring in the region. However, examination of the results from both grid systems did not yield any significant differences (ref. 7). Since the 26 body model could be run at a larger time step, and therefore require less computer time, it was used for most of the analysis.

Table 1. One-dimensional model

1st Grid (26 bodies)			2nd Grid (31 bodies)		
	Node Number	Thickness (in.)		Node Number	Thickness (in.)
	1	.002		1,2	.001
	2 to 10	.004		3 to 20	.002
(interface)	11	.002	(interface)	21	.004
	12	.004		22	.004
	13	.008		23	.008
	14	.012		24	.012
	15	.020		25	.024
	16 to 25	.040		26,27,28	.05
	26	.054		29,30,31	.1

Two-Dimensional Model

Although one-dimensional modeling is adequate for most of the folded geometry thermal analysis, certain regions require two-dimensional studies. The web, or interpose region near the breech end, will experience two-dimensional heating. To analyze this region, an isothermal model, shown in figure 7, has been developed. This model consists of 62 bodies, with 50 bodies in the cartridge case. Initially a smaller model consisting of 37 bodies, with 25 bodies in cartridge case, was considered. However, nodalization studies showed that this grid was too large. Because of the symmetry in the web, only half of the web was modeled. The rectangular region is 0.23 in. by 0.56 in. and contains the web region up to the base of the projectile.

The computer program used to analyze the two-dimensional problem is essentially the same as the one described in the One-Dimensional Model section. The major difference is that surface and

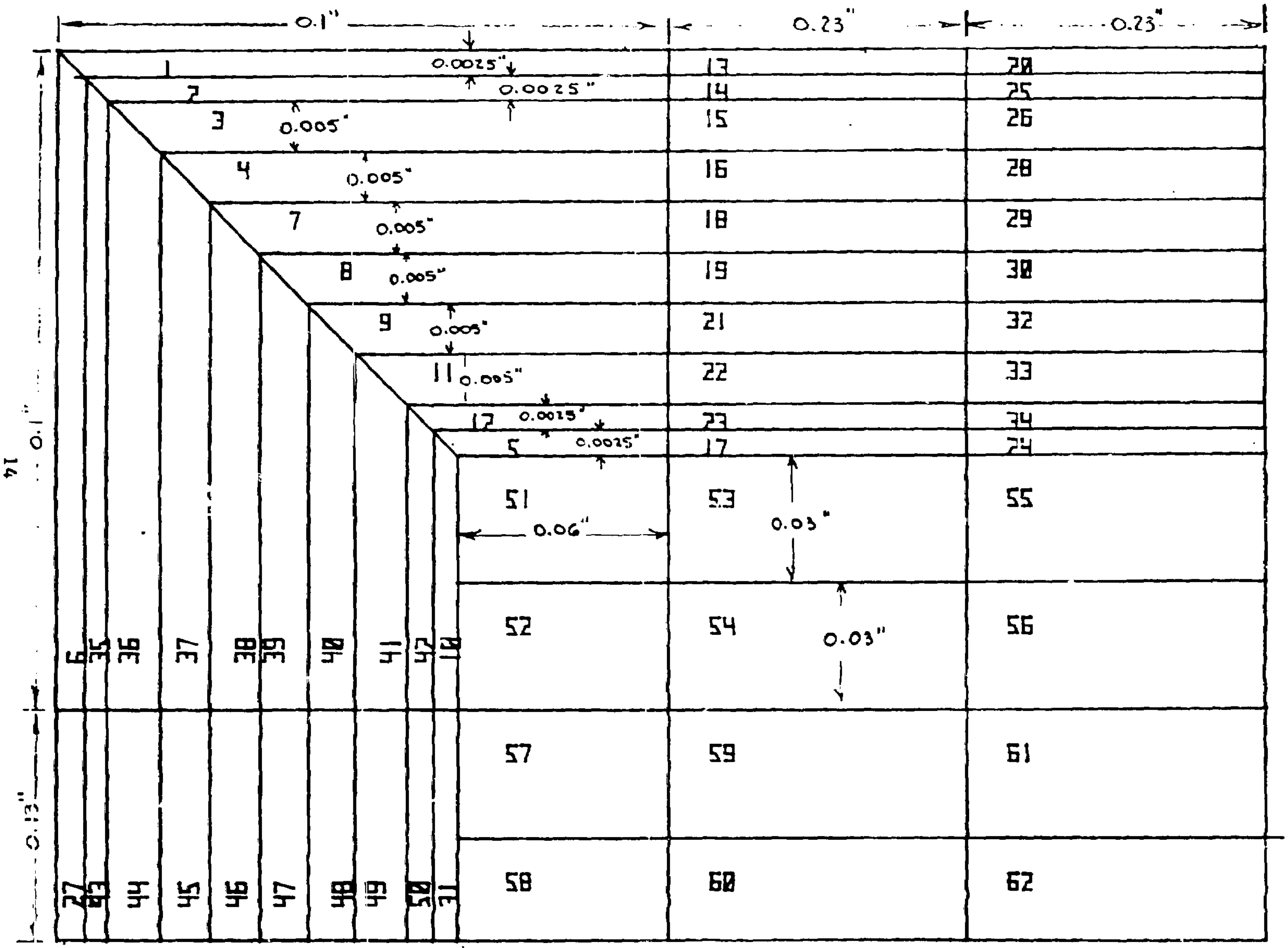

Figure 7. Two dimensional model.

interior nodes are identified, and surface nodes are allowed to experience convection. Appendix B contains the Fortran listing of the program.

RESULTS

One-Dimensional

Using the one-dimensional model described previously, temperature profiles have been determined for 29 cycles or rounds.

During any cycle, the surface of the cartridge exposed to the hot gases experiences a rapid temperature rise, with the peak occurring at approximately 2 msec. Figures 8 through 11 present the surface temperature history for rounds 1, 10, 20, and 29. These profiles are similar, with the peak temperature reaching a maximum value of approximately 1346°F. The sharp drop in temperature, occurring at 65 msec, results from the extraction of the spent round and the insertion of an unspent cartridge with the cartridge case at 100°F. The unspent cartridge is then heated by the warmer weapon chamber. Figure 12 presents a composite of the profile for rounds 1, 10, 20, and 29. From this figure it can be seen that by the tenth round, the surface temperature profile is stabilized. Figure 13 presents the peak surface temperature as a function of round number. It would appear that by round 4, the peak surface temperature has reached equilibrium at approximately 1345°F. However, examination of the detailed computer printouts shows that between rounds 19 and 29, the peak surface temperature rose 0.5°F. This rate, of course, is decreasing with each round, but extrapolation would yield a conservative estimate of the peak temperature after a one minute burst of 600 rounds. Using a rate of 1°F per 20 rounds, the extrapolated peak surface temperature is 1374°F.

During the ballistic portion of any firing cycle, there is very little penetration of the thermal wave into the weapon chamber. Reference 7 states that at the conclusion of the ballistic period (approximately 3.5 msec), the interface between the cartridge case and steel portion of the weapon experienced less than a 1°F rise. Over the 100 msec firing cycle, however, the thermal wave does penetrate into the steel structure. Figures 14 through 17 present the temperature distribution across the model at the end of the cycle for rounds 1, 10, 20, and 29. After 20 rounds, the temperature rise in the steel, at a depth of 0.25 in., is still less than 20°F. Figure 18 presents a composite of figures 14 through 17. From this figure, the propagation of the thermal wave can be seen. The peak temperature shown in figure 18 is not the highest steel temperature, but rather the condition existing at the end of the cycle for a particular round. Figure 19 presents the peak interface temperature as a function of round number. This represents the maximum steel

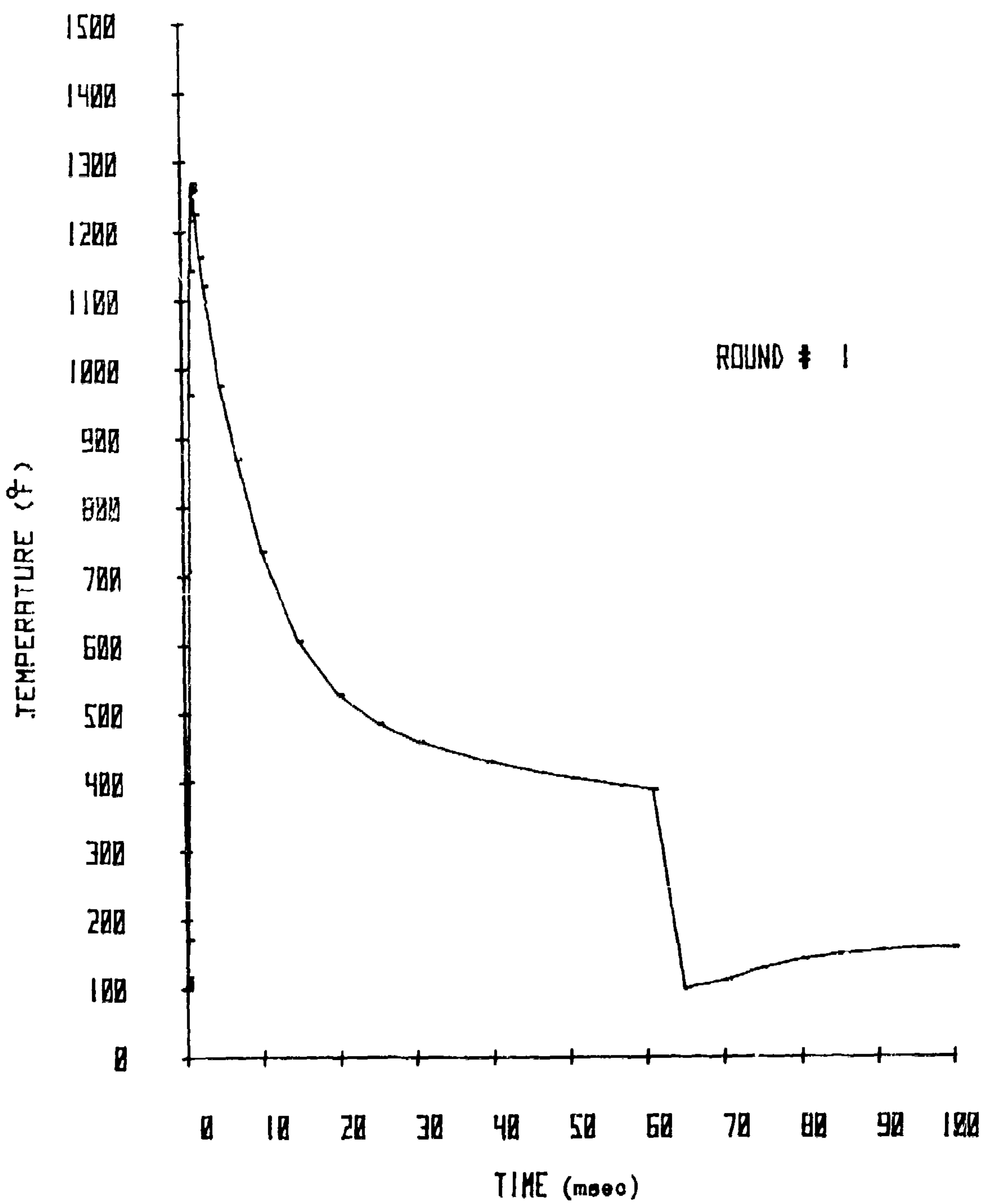

Figure 8. Surface temperature versus time, round 1.

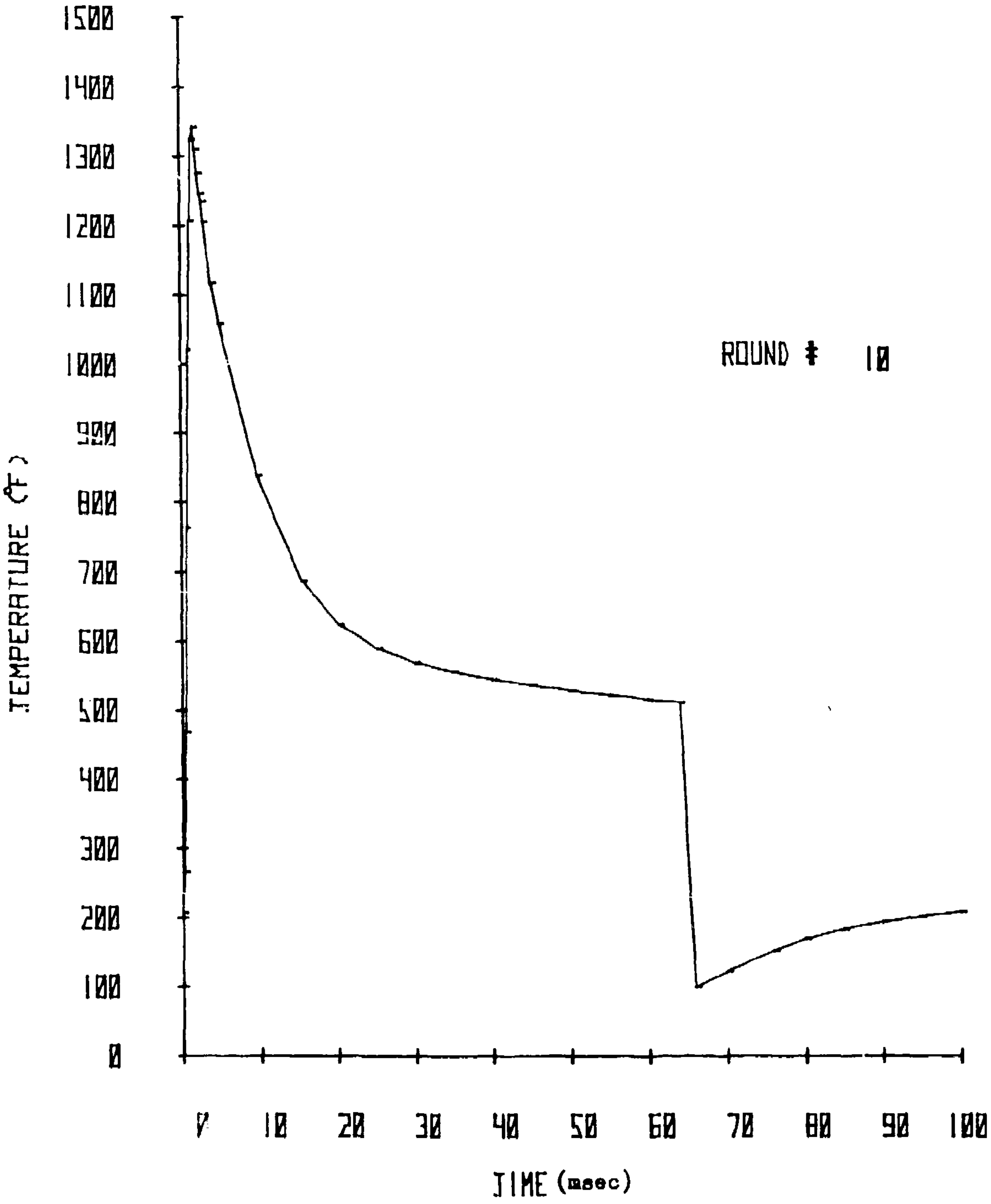

Figure 9. Surface temperature versus time, round 10.

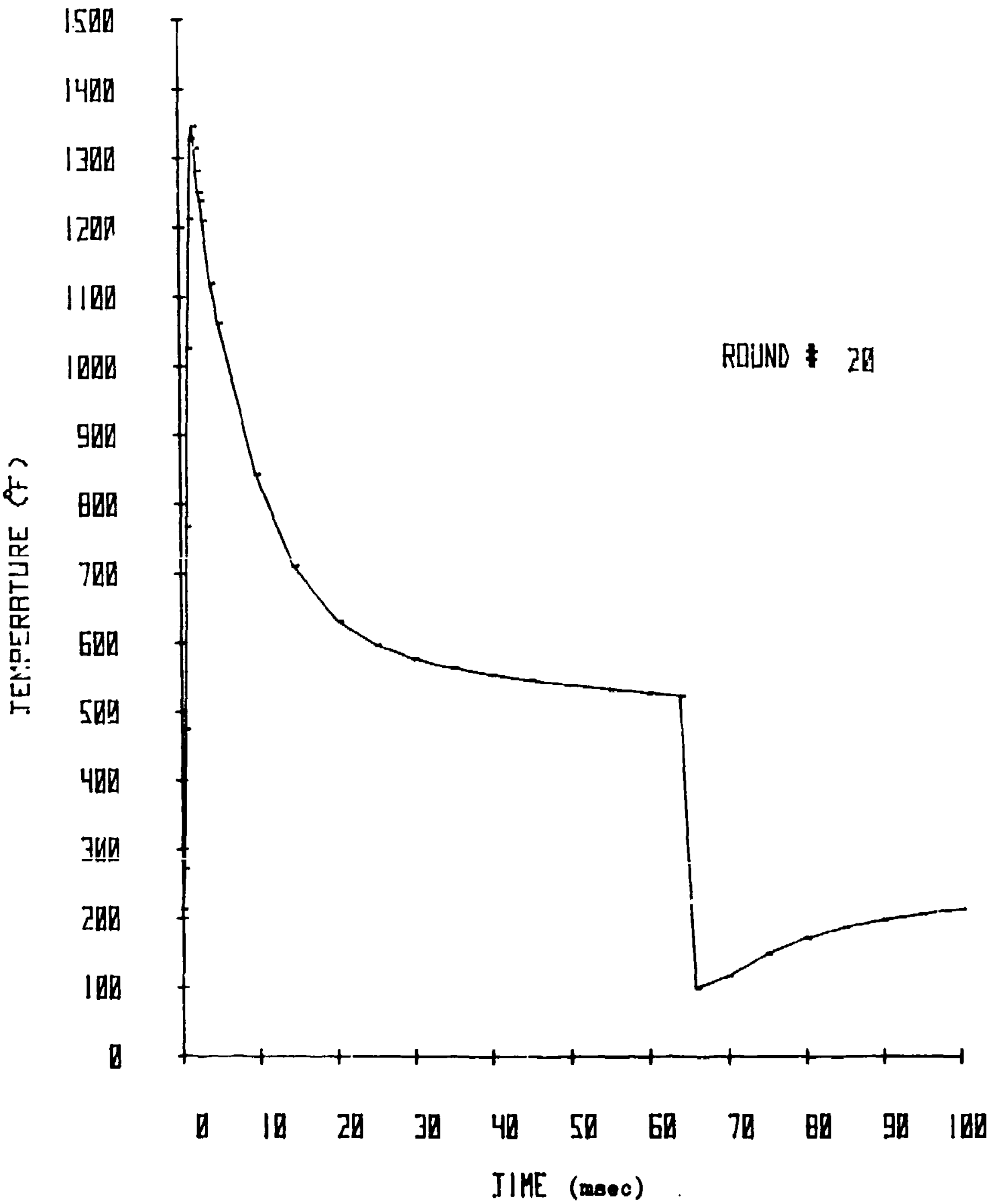

Figure 10. Surface temperature versus time, round 20.

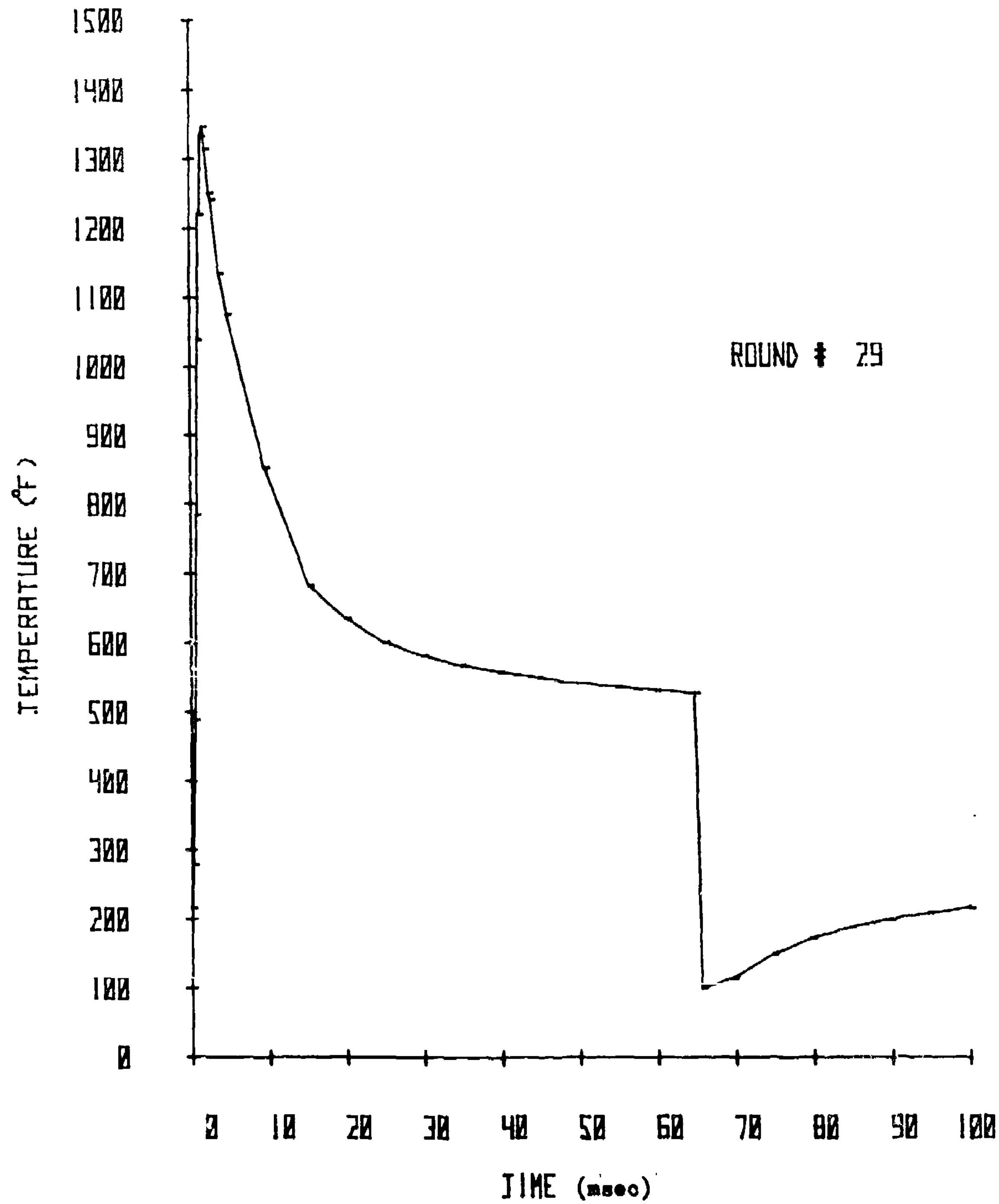

Figure 11. Surface temperature versus time, round 29.

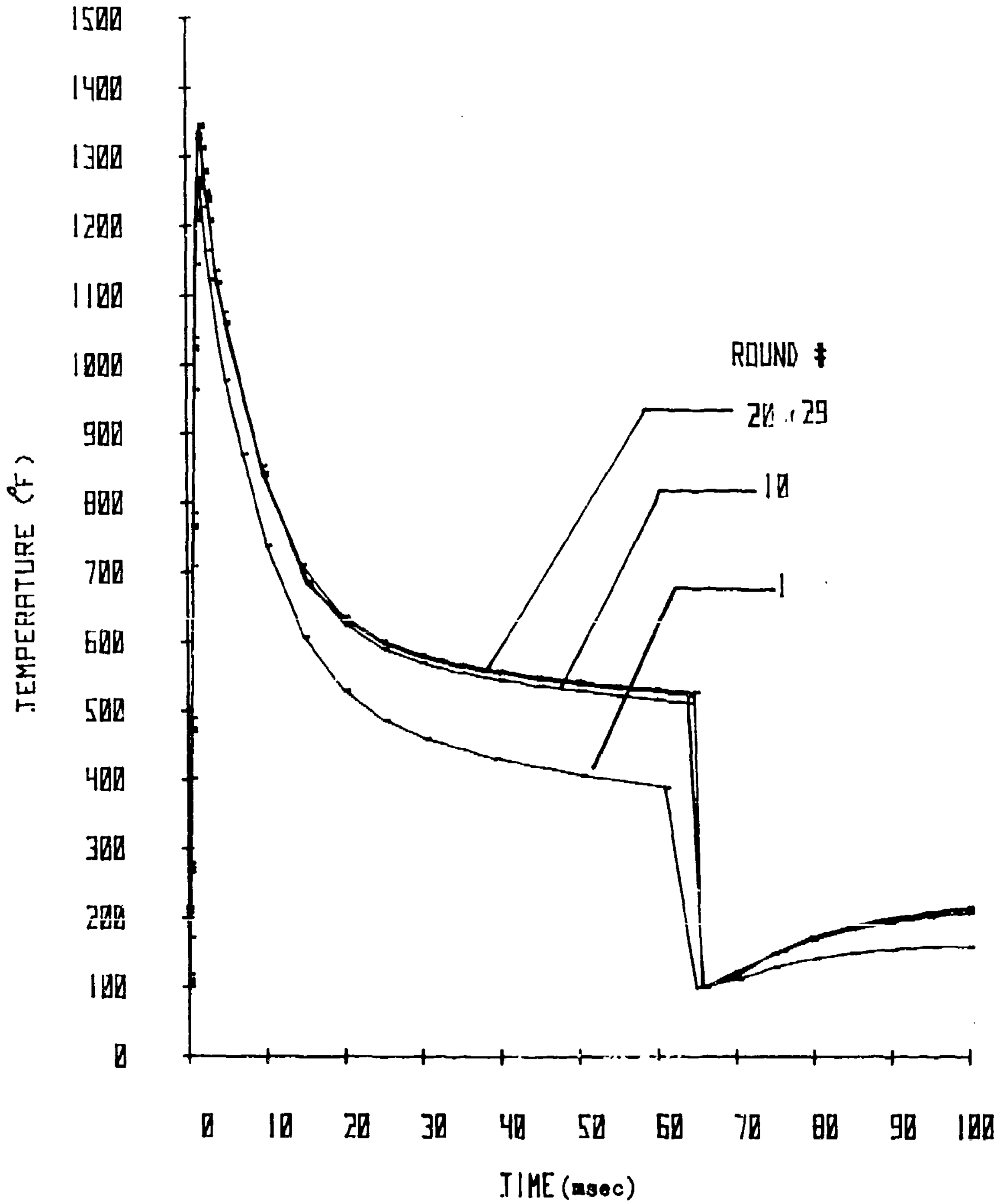

Figure 12. Surface temperature versus time, rounds 1, 10, 20 & 29.

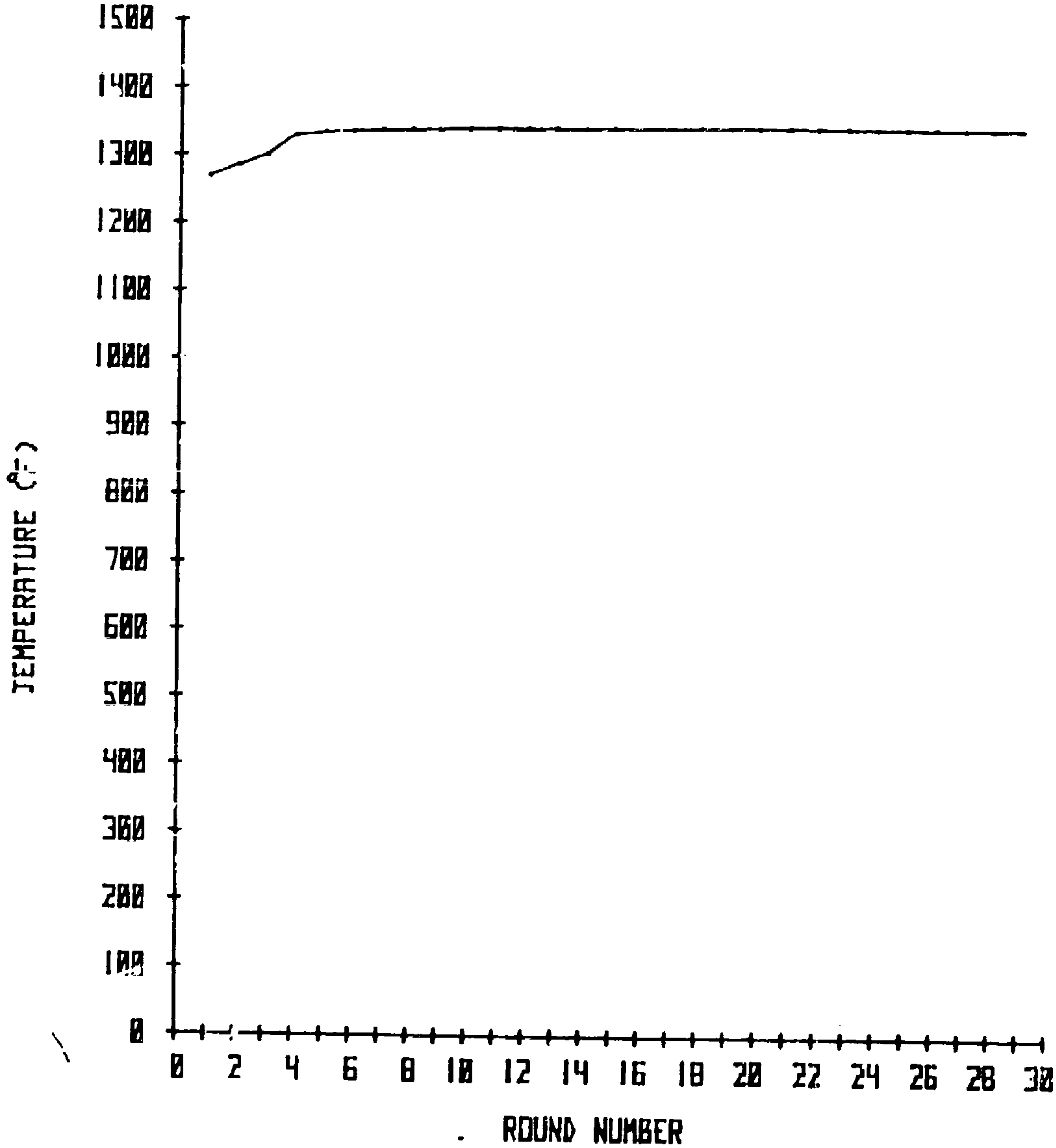

Figure 13. Peak surface temperature versus round number.

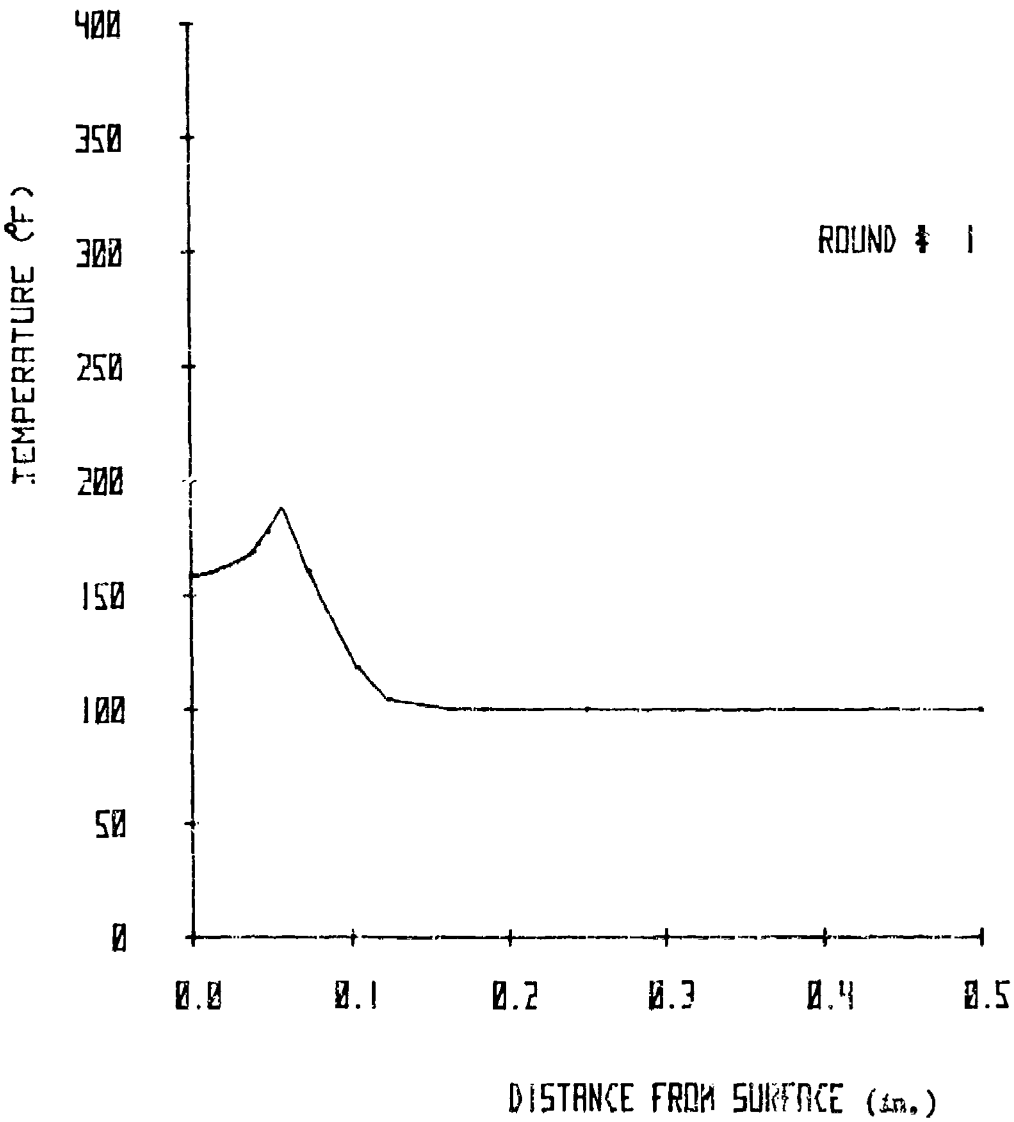

Figure 14. Temperature versus distance at 100 (msec).

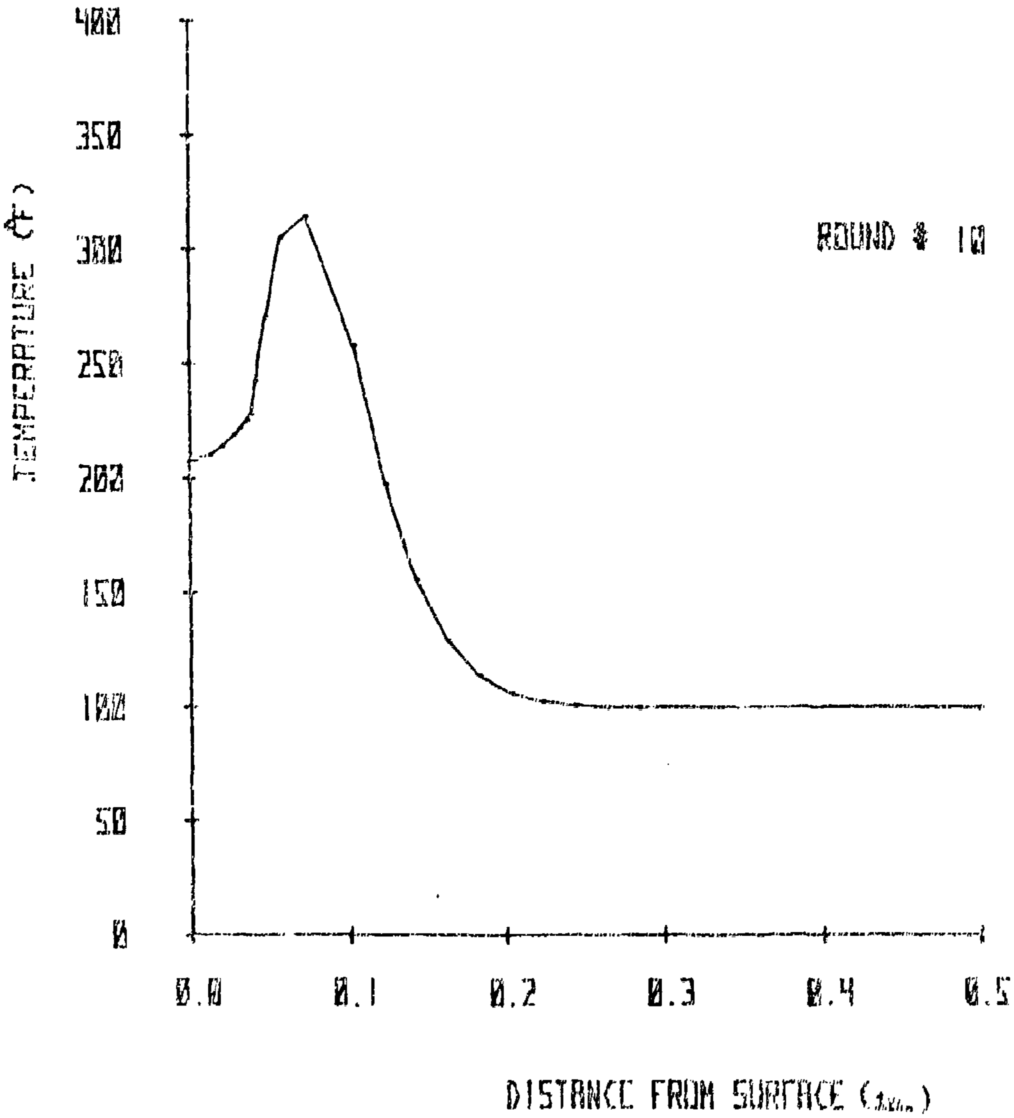

Figure 15. Temperature versus distance at 1000 (msec).

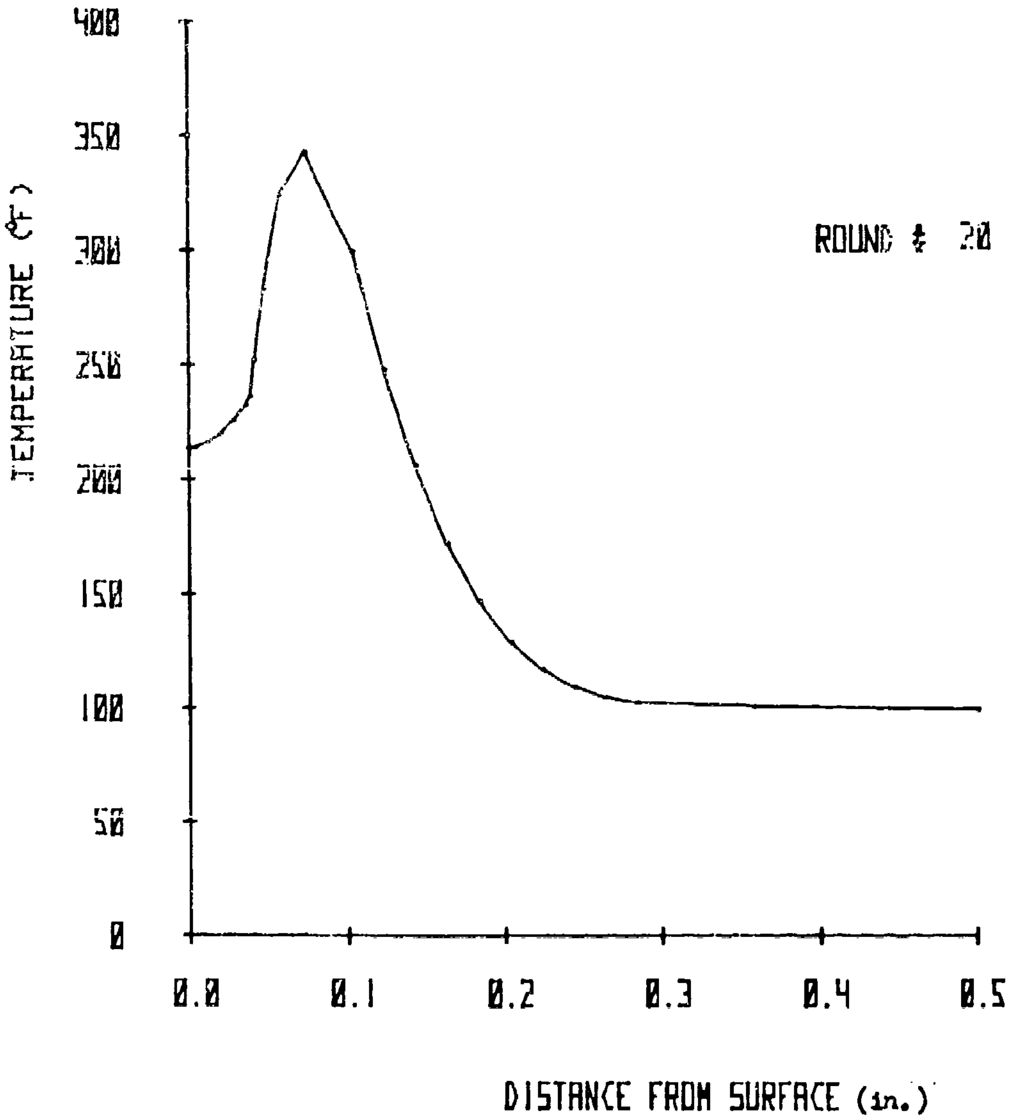

Figure 16. Temperature versus distance at 2000 (msec).

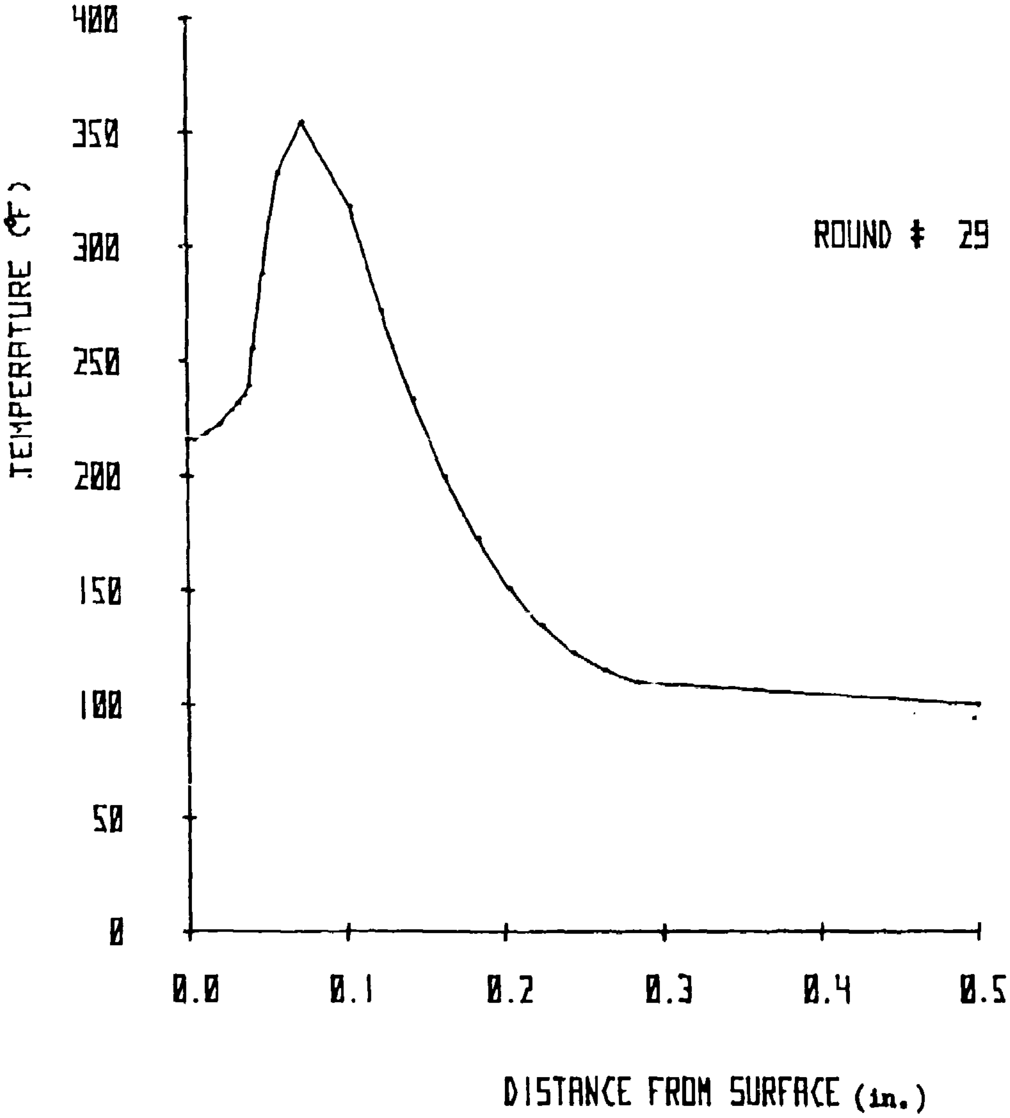

Figure 17. Temperature versus distance at 2900 (msec).

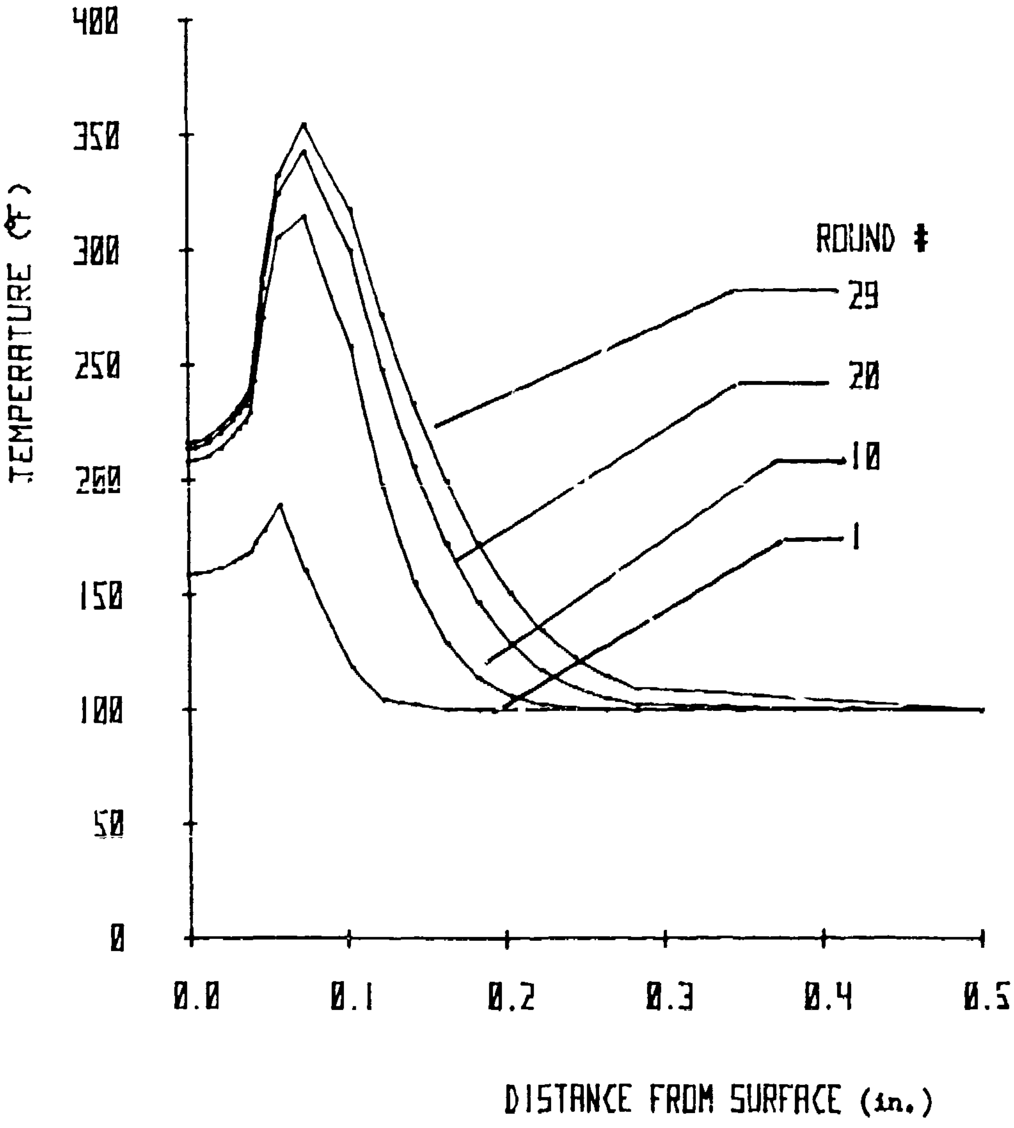

Figure 18. Temperature versus distance.

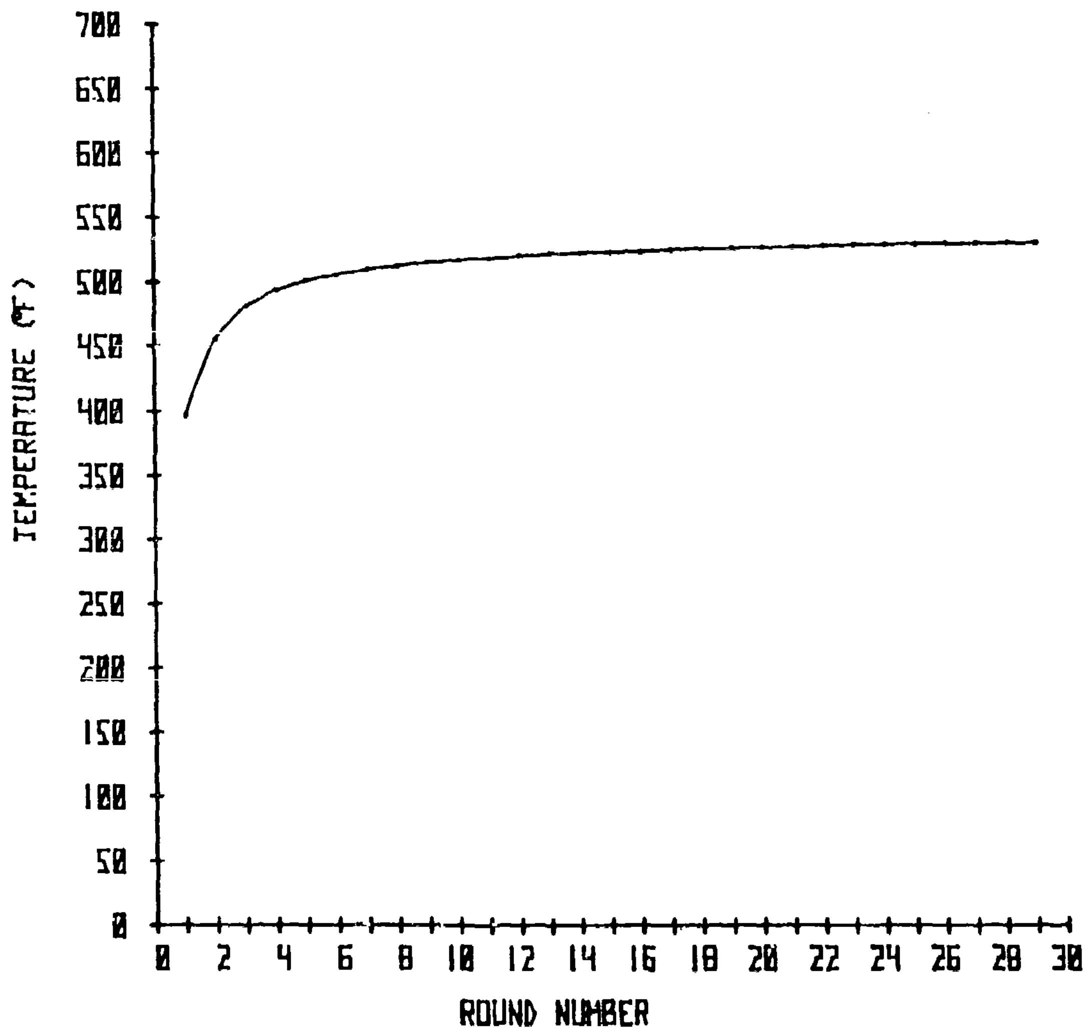

Figure 19. Peak interface temperature versus round number.

temperature. The peak temperature is still increasing at the rate of 0.3°F per round at round 29. Extrapolation of this rate out to 600 rounds is very dangerous. It would result in a peak steel temperature of approximately 700°F. This is an unrealistically high value. In addition, the question of depth of penetration must be considered. Examination of figure 18 shows that a 100°F temperature rise over the initial temperature has penetrated only 25% of the steel thickness. During future studies, additional cycles would be run.

The results of the one-dimensional analysis show that the penetration of the thermal wave is very slow, and therefore in those regions where this analysis is valid, conditions for the folded geometry are no worse than for conventional ammunition. In addition, since the severe heating during the ballistic phase is very short, this environment will heat the weapon uniformly and result in one-dimensional heat flow. A major factor affecting the structural temperature is the timing of the firing cycle. A shorter dwell time would greatly reduce the peak temperatures.

The major effect of the folded geometry is evidenced at the small interpose region near the base of the projectile. In this region the two-dimensional effect may be significant. The following section presents the two-dimensional results obtained for this region.

Two-Dimensional

Temperature distributions have been obtained for the model, and are described in the Two-Dimensional Model Section. The region examined is the base of the interpose region near the projectile base. Since the heating is uniform, only half of the web has to be considered. Figures 20 through 23 present the peak temperature occurring in this region for 4 complete cycles. The peak surface temperature in the corner is slightly higher than the peak temperature for the one-dimensional analysis. However, the temperature difference is approximately 1%, well within the accuracy of the analytical model. In figure 23, to the right of the model, the maximum temperatures corresponding to the same approximate location in the steel are given. For instance, the maximum interface temperature for round 4, node 24, in the one-dimensional analysis, is 493°F. The highest two-dimensional interface temperature at node 10 is 628°F. Node 10 is in the corner. However, node 24, located 0.41 in. from the corner, has a maximum of 521°F, as compared to 493°F in the one-dimensional interface temperature.

The results obtained from the two-dimensional calculations indicate that the temperature will be higher near the base of the interpose region. However, this level, at least after 4 rounds, is not prohibitive. In evaluating the temperature profiles, it will be necessary to assess the structural effect of small penetrations of high temperatures into the steel. This would be a major part of future efforts.

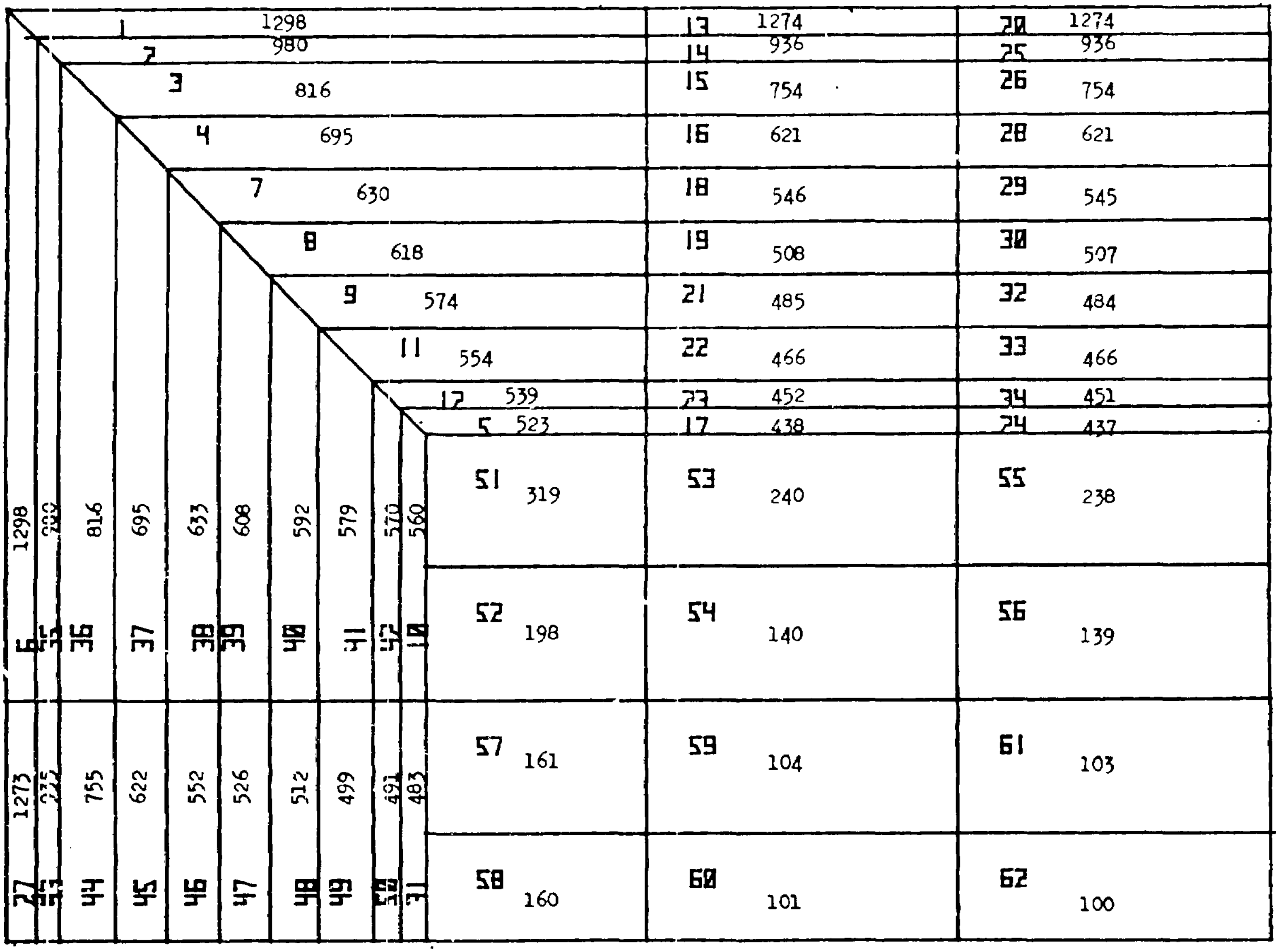

Figure 20. Peak temperatures for round 1 (°F)

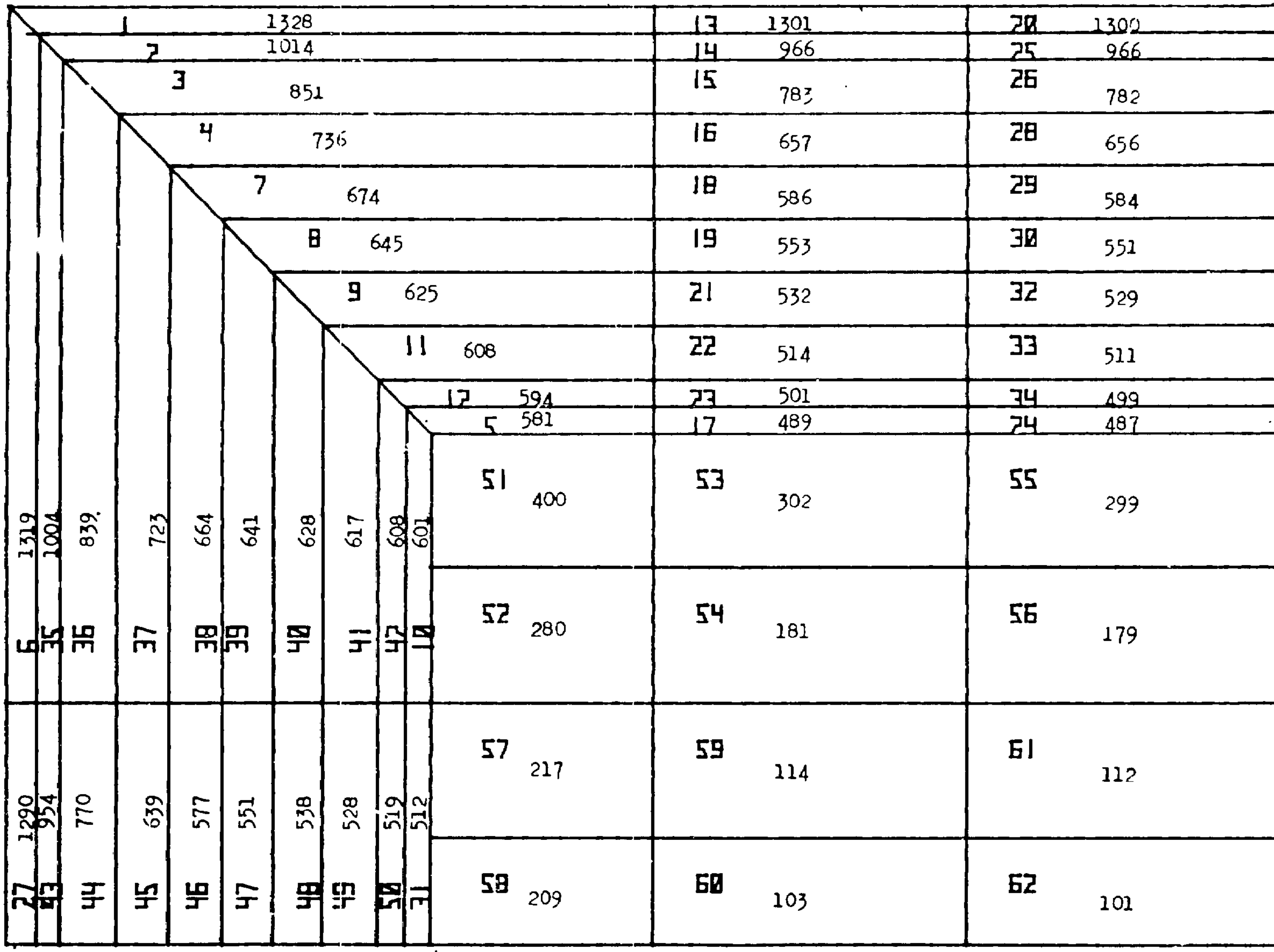

Figure 21. Peak temperatures for round 2 (°F).

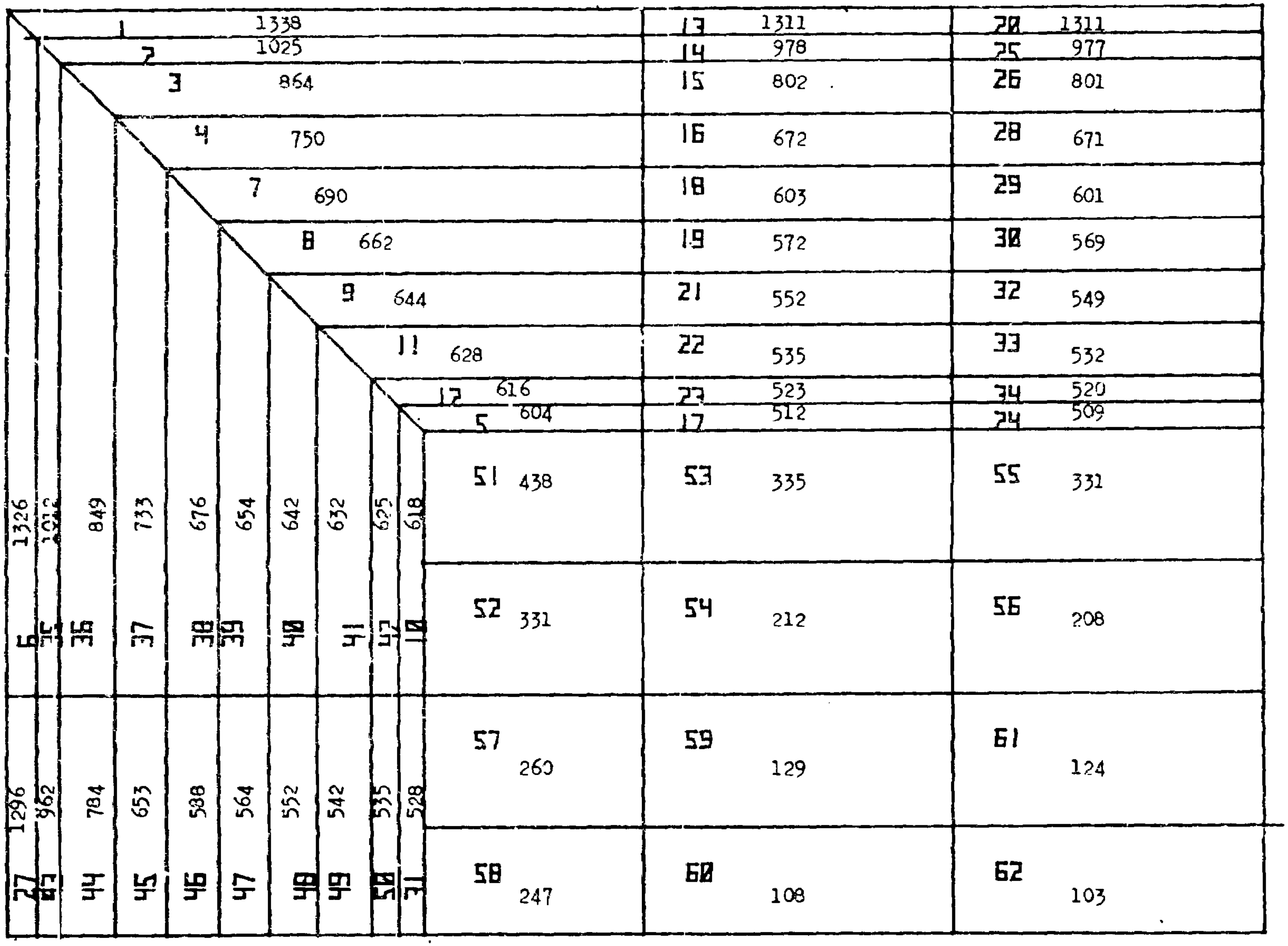

Figure 22. Peak temperatures for round 3 (°F).

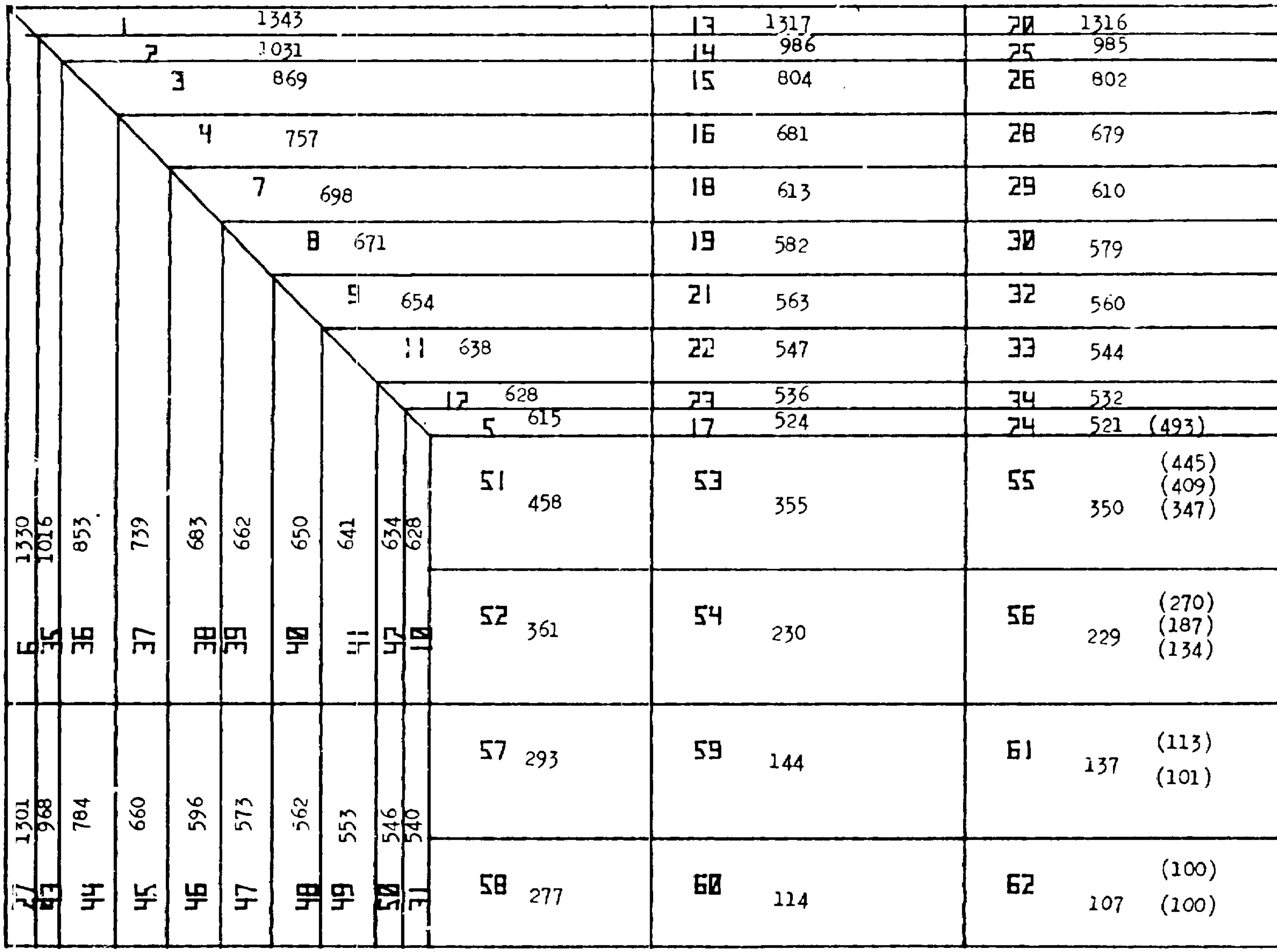

Figure 23. Peak temperatures for round 4 (^{o}F).

CONCLUSIONS

The thermal response of the folded geometry cartridge has been determined for one and two-dimensional models, and also for single and multiple firings. The results show that the surface of the cartridge case heats very rapidly due to the propellant combustion. The one-dimensional model has been run for 29 rounds, and the two-dimensional model for 4 rounds.

The peak cartridge case temperature occurs at the base of the interpose region, based upon two-dimensional calculations. At round 4, this peak is 1343°F. For the one-dimensional model, the corresponding peak is 1331°F. The two-dimensional effect on peak cartridge temperature is therefore very small. Extrapolating the one-dimensional results to 600 rounds would yield a peak of 1370°F. By applying the same difference of approximately 1.0%, for the worst two-dimensional results, the peak cartridge temperature would be less than 1400°F after 600 rounds. This result would indicate that with respect to peak cartridge temperature, the folded geometry cartridge is no worse than conventional rounds.

With respect to the weapon chamber, the interface temperature at the base of the interpose region will be hotter, due to the folded geometry. After 4 rounds, the peak interface temperature is 628°F for the two-dimensional analysis, compared to 493°F for the one-dimensional analysis. Extrapolation of these results, to conditions after 600 rounds, is not possible at this time. However, it seems reasonable to conclude that the base of the interpose region will experience more severe temperatures than would exist with conventional ammunition.

Future effort should concentrate on additional firings with the two-dimensional model, an investigation of the heating cycle during the period after the ballistic portion of the cycle, and thermal stress calculations of the effect of thermal distortion and elevated temperatures upon material strength.

REFERENCES

1. T. R. Trafton, "An Improved Interior Ballistic Model for Small Arms Using Deterred Propellants," USA Ballistic Research Laboratories, BRL R 1624, Nov. 1972.

2. Sidney Goldstein, "A Simplified Model for Predicting the Burning Rate and Thermochemical Properties of Deterred Rolled Ball Propellant." U.S. Army Armament Command, Frankford Arsenal, TN-1184, December 1973.

3. N. E. Banks, and G. J. Klem, "A Study of Heat Transfer in Folded Ammunition Gun Tube Chambers," BRL 1, November 1976.

4. T. J. Dahm, and L. W. Anderson, "Propellant Gas Convective Heat Transfer in Gun Barrels," Aerotherm Corp. (Rock Island Arsenal), SWERR-TR-72-43, June 1972.

5. Saha Pradip, "An Analytical Study of the Interior Ballistic Problem Including Movement of Solids and Wall Heat Transfer," M. S. Thesis, Georgia Institute of Technology, September 1971.

6. A. Peretz, K. K. Koo, L. H. Cavney, and M. Summerfield, "Starting Transient of Solid-Propellant Rocket Motors with High Internal Gas Velocities," AIAA Journal, Vol. 11, No. 12, December 1973, pp 1729-1727.

7. E. V. McAssey, "Heat Transfer of the Folded Cartridge Phase II Report," June 1978.

APPENDIX A

ONE-DIMENSIONAL PROGRAM LISTING

```
// JOB MCASSEY,3610****10/****,CLASS=L(F2)                                    DATE 06/12/78,CLOCK 13/2
// EXEC WATFIV,SIZE=0256K

      /PROGRAM MCASSEY,PAGES=500,TIME=15
      C
      C
      C
      C    **********  ONE DIMENSIONAL THERMAL ANALYSIS PROGRAM  *************
      C
      C
      C
      C
            REAL M
            DIMENSION TFREE(50),FILM(50),TIME(50),M(100),C(100),AREA(100),TI(1
           100),COND(100,100),TEMP(100),TNEW(100)
            READ (5,1000) DELTA,NBODY,NCOUP,N
            DELTA=DELTA/3600.
            WRITE (6,2002) DELTA,NBODY,NCOUP,N
            READ(5,1002)ICT,INC,INTER,CDEL
            CDEL=CDEL/3600.
            WRITE(6,2008)ICT,INC,INTER,CDEL
            READ (5,1001)(TFREE(I),FILM(I),TIME(I),I=1,N)
            PRINT=1.35E-07
            PRC=0.0
            DO 4 I=1,N
            TFREE(I)=TFREE(I)-460.0
          4 TIME(I)=TIME(I)/3600.0
            WRITE (6,2003)
            WRITE(6,2004)(TFREE(I),FILM(I),TIME(I),I,I=1,N)
            DO 5 I=1,NBODY
          5 READ (5,1005) M(I),C(I),AREA(I),TI(I)
            DO 6 I=1,NBODY
            DO 6 J=1,NBODY
          6 COND(I,J)=0.0
            DO 10 K=1,NCOUP
            READ (5,1007) I,J,COND(I,J)
            COND(J,I)=COND(I,J)
         10 CONTINUE
            DO 15 I=1,NBODY
            WRITE(6,3000)I
            WRITE(6,2005) M(I),C(I),AREA(I),TI(I)
            DO 15 J=1,NBODY
            IF(COND(I,J).GT.0.0) WRITE (6,2007)I,J,COND(I,J)
         15 CONTINUE
            MLIM=N-1
            TT=TIME(1)*3.6E06
            DO 16 I=1,NBODY
         16 TNEW(I)=TI(I)
            WRITE (6,3000) TT
            WRITE (6,3001)(J,TI(J),J=1,NBODY)
            DO 500 IT=1,MLIM
            IF(IT.EQ.ICT) DELTA=CDEL
            IF(IT.EQ.ICT) PRINT=9.6*DELTA
            IF(IT.EQ.INC) GO TO 40
            GO TO 42
         40 JC=INTER-1
            DO 41 I=1,JC
         41 TNEW(I)=100.
         42 CONTINUE
            WORK=TIME(IT+1)-TIME(IT)
            IF(WORK.EQ.0.00) GO TO 500
            SLOPE=(TFREE(IT+1)-TFREE(IT))/WORK
            HSLOP=(FILM(IT+1)-FILM(IT))/WORK
            TSTOP=TIME(IT+1)
            TSTART=TIME(IT)
```

```
      TT=TSTART
   50 TT=TT+DELTA
      IF(TT.GT.TSTOP) TT=TSTOP
      DO 52 I=1,NBODY
      TEMP(I)=TNEW(I)
   52 CONTINUE
      DO 100 I=1,NBODY
   56 WORK=DELTA/M(I)/C(I)
      IF (I.GT.1) GO TO 60
      SUM=WORK*AREA(I)*(FILM(IT)+HSLOP*(TT-TSTART))*(TFREE(IT)+SLOPE*(TT
     1-TSTART))
      GO TO 61
   60 SUM=0.0
   61 SUM1=0.0
      DO 70 J=1,NBODY
      SUM1=SUM1+COND(I,J)
      SUM=SUM+WORK*COND(I,J)*TEMP(J)
   70 CONTINUE
      IF(I.GT.1) GO TO 75
      TNEW(I)=SUM+(1.-WORK*(SUM1+AREA(I)*(FILM(IT)+HSLOP*(TT-TSTART))))
     1*TEMP(I)
      IF(TNEW(I).LT.50) WRITE(6,3003)
      IF(TNEW(I).LT.50) STOP
      GO TO 100
   75 TNEW(I)=SUM+(1-WORK*SUM1)*TEMP(I)
      IF(TNEW(I).LT.50) WRITE(6,3003)
      IF(TNEW(I).LT.50) STOP
  100 CONTINUE
      TTT=TT*3.6E6
      PRC=PRC+DELTA
      IF (PRC.LT.PRINT) GO TO 102
      PRC=0.0
      WRITE (6,3000) TTT
      WRITE (6,3002)
      WRITE (6,3001) (J,TNEW(J),J=1,NBODY)
  102 CONTINUE
      IF(TT.EQ.TSTOP) GO TO 500
      GO TO 50
  500 CONTINUE
      WRITE (6,3000) TTT
      WRITE (6,3002)
      WRITE (6,3001) (J,TNEW(J),J=1,NBODY)
      WRITE (7,4000)  (M(I),C(I),AREA(I),TNEW(I),I=1,NBODY)
      STOP
 1000 FORMAT (E20.5,3I4)
 1001 FORMAT (3F20.5)
 1005 FORMAT(4E20.5)
 1007 FORMAT (2I5,F10.5)
 2002 FORMAT (1H1,'TIME STEP=',E20.5,2X,'HRS',5X,'NUMBER OF BODIES=',I4,
     120X,'ANALYSIS BASED ON 1 ST GRID SYSTEM',
     1/1X,'NUMBER OF COUPLINGS=',I4,5X,'NUMBER OF TIME INTERVALS=',I4)
 2003 FORMAT(1H0,15X,'HEAT INPUT PROFILE',//1X,'FREE STREAM TEMP (F)',10
     $X,'HEAT TRANSFER COEFF',10X,'TIME (HRS)',5X,'TIME INTERVAL')
 2004 FORMAT(1H0,5X,F8.2,20X,E10.3,10X,E10.3,10X,I3)
 2006 FORMAT (5X,4E20.5)
 2007 FORMAT (2I5,5X,F15.5)
 3000 FORMAT (1H0,'TIME=',E14.5,'MILLISEC')
 3001 FORMAT (1H0,(I4,2X,E12.4,3X))
 3002 FORMAT (1X,'BODY #',2X,'NEW TEMP')
 3003 FORMAT (1X,'TNEW IS LESS THAN 50 DEGREES. PROGRAM TERMINATED ')
 4000 FORMAT (4E20.5)
 1002 FORMAT(3I2,E20.5)
 2008 FORMAT(1H0,'TIME STEP CHANGE AT N=',I2,/1X,'NEW CARTRIDGE ATN=',I2
```

```
     $,/1X,'INTERFACE AT BODY NODE',I2,/1X,'NEW TIME STEP=',E20.5)
3600 FORMAT(1X,'BODY NUMBER=',I5)
     END

/GO
```

APPENDIX B

TWO-DIMENSIONAL PROGRAM LISTING

```
// JOB MCASSEY,3610****10/****,CLASS=L(F2)                                   DATE 06/12/78,CLOCK 13/4
// EXEC WATFIV,SIZE=0256K

       /PROGRAM MCASSEY,PAGES=500,TIME=6
       C
       C
       C
       C          **********  TWO DIMENSIONAL TEMPERATURE PROGRAM   ****
       C
       C
       C
                  REAL M
                  DIMENSION TFREE(20),FILM(20),TIME(20),M(100),C(100),AREA(100),TI(1
                 100),COND(100,100),TEMP(100),TNEW(100)
                  DIMENSION ITYPE(100)
                  READ (5,1000) DELTA,NBODY,NCOUP,N
                  WRITE (6,2002) DELTA,NBODY,NCOUP,N
                  READ (5,1001)(TFREE(I),FILM(I),TIME(I),I=1,N)
                  PRINT=.675E-07
                  PRC=0.0
                  DO 4 I=1,N
                  TFREE(I)=TFREE(I)-460.0
                4 TIME(I)=TIME(I)/3600.0
                  WRITE (6,2003)
                  WRITE (6,2004)(TFREE(I),FILM(I),TIME(I),I=1,N)
                  DO 5 I=1,NBODY
                5 READ (5,1005) M(I),C(I),AREA(I),TI(I),ITYPE(I)
                  DO 6 I=1,NBODY
                  DO 6 J=1,NBODY
                6 COND(I,J)=0.0
                  DO 10 K=1,NCOUP
                  READ (5,1007) I,J,COND(I,J)
                  COND(J,I)=COND(I,J)
               10 CONTINUE
                  DO 15 I=1,NBODY
                  WRITE(6,3600)I
                  WRITE(6,2006) M(I),C(I),AREA(I),TI(I),ITYPE(I)
                  DO 15 J=1,NBODY
                  IF(COND(I,J).GT.0.0) WRITE (6,2007)I,J,COND(I,J)
               15 CONTINUE
                  MLIM=N-1
                  TT=TIME(1)*3.6E06
                  DO 16 I=1,NBODY
               16 TNEW(I)=TI(I)
                  WRITE (6,3000) TT
                  WRITE (6,3001)(J,TI(J),J=1,NBODY)
                  DO 500 IT=1,MLIM
                  WORK=TIME(IT+1)-TIME(IT)
                  SLOPE=(TFREE(IT+1)-TFREE(IT))/WORK
                  HSLOP=(FILM(IT+1)-FILM(IT))/WORK
                  TSTOP=TIME(IT+1)
                  TSTART=TIME(IT)
                  TT=TSTART
               50 TT=TT+DELTA
                  IF(TT.GT.TSTOP) TT=TSTOP
                  DO 52 I=1,NBODY
                  TEMP(I)=TNEW(I)
               52 CONTINUE
                  DO 100 I=1,NBODY
                  WORK=DELTA/M(I)/C(I)
                  IF(ITYPE(I).EQ.1) GO TO 60
                  SUM=WORK*AREA(I)*(FILM(IT)+HSLOP*(TT-TSTART))*(TFREE(IT)+SLOPE*(TT
                 1-TSTART))
                  GO TO 61
               60 SUM=0.0
```

```
   61 SUM1=0.0
      DO 70 J=1,NBODY
      SUM1=SUM1+COND(I,J)
      SUM=SUM+WORK*COND(I,J)*TEMP(J)
   70 CONTINUE
      IF(ITYPE(I).EQ.1) GO TO 75
      TNEW(I)=SUM+(1.-WORK*(SUM1+AREA(I)*(FILM(IT)+HSLOP*(TT-TSTART))))
     1*TEMP(I)
      IF(TNEW(I).LT.50.) STOP
      IF(TNEW(I).LT.50.) WRITE(6,3500)
      GO TO 100
   75 TNEW(I)=SUM+(1-WORK*SUM1)*TEMP(I)
      IF(TNEW(I).LT.50.) WRITE(6,3500)
      IF(TNEW(I).LT.50.) STOP
  100 CONTINUE
      TTT=TT*3.6E06
      PRC=PRC+DELTA
      IF (PRC.LT.PRINT) GO TO 102
      PRC=0.0
      WRITE (6,3000) TTT
      WRITE (6,3002)
      WRITE (6,3001) (J,TNEW(J),J=1,NBODY)
  102 CONTINUE
      IF(TT.EQ.TSTOP) GO TO 500
      GO TO 50
  500 CONTINUE
      WRITE (6,3000) TTT
      WRITE (6,3002)
      WRITE (6,3001) (J,TNEW(J),J=1,NBODY)
      WRITE (7,4000)  (M(I),C(I),AREA(I),TNEW(I),I=1,NBODY)
      STOP
 1000 FORMAT (E20.5,3I4)
 1001 FORMAT (3F20.5)
 1005 FORMAT(4F10.5,I2)
 1007 FORMAT (2I5,F10.5)
 2002 FORMAT (1H1,'TIME STEP=',E20.5,5X,'NUMBER OF BODIES=',I4,/1X,'NUMB
     1ER OF COUPLINGS=',I4,5X,'NUMBER OF TIME INTERVALS=',I4)
 2003 FORMAT(1H0,15X,'HEAT INPUT PROFILE',//1X,'FREE STREAM TEMP',10X,'H
     1EAT TRANSFER COEFF',10X,'TIME')
 2004 FORMAT (1H0,5X,F8.2,20X,E10.3,10X,E10.3)
 2006 FORMAT(5X,4E20.5,I2)
 2007 FORMAT (2I5,5X,F15.5)
 3000 FORMAT (1H0,'TIME=',E14.5,'MILLISEC')
 3001 FORMAT (1H0,(I4,2X,E12.4,3X))
 3002 FORMAT (1X,'BODY #',2X,'NEW TEMP')
 3500 FORMAT(1X,'TEMPERATURE BELOW 50')
 3600 FORMAT(1X,'BODY NUMBER  ',I5)
 4000 FORMAT (4E20.5)
      END

/GO
```

DISTRIBUTION LIST

Defense Documentation Center
Cameron Station
ATTN: DDA-2 (10)
Alexandria, VA 22314

Office of the Deputy Undersecretary of Defense
Research and Engineering
Pentagon Room 3D1098
ATTN: Mr. R. Thorkildson
Washington, DC 20301

AMRAD/USDDR&E
Pentagon
Washington, DC 20301

Commander
Headquarters Army Material Development & Readiness Command
5001 Eisenhower Avenue
ATTN: DRCDE-DH, COL E. Shore
DRCIRD, COL R. Cuthbertson
DRCDE-DA, LTC A. Collins
DRCDE-DG, Mr. T. Cosgrove
DRCIRD Mr. B. Dunetz
Alexandria, VA 22333

Commander
Combined Arms Center
ATTN: ATCA-COF, LTC R. Sellers
Ft. Leavenworth, KS 66048

Commanding General
Training and Doctrine Command
ATTN: Library Bldg. 133
Ft. Monroe, VA 23651

Director
US Army Training and Doctrine Command
Systems Analysis Activity
ATTN: ATAA-SL, Technical Library
White Sands Missile Range, NM 88002

Commander
Army Missile Command
ATTN: DRSMI-AOM
RDIMI-R
Redstone Arsenal, AL 35809

Commanding General
US Army Air Defense School
P.O. Box 5040
ATTN: Technical Library
Ft. Bliss, TX 79916

Assistant Commandant
US Army Armor School
ATTN: Technical Library
Ft. Knox, KY 40121

Commandant
US Army Field Artillery School
ATTN: Morris Swett Library
Ft. Sill, OK 73503

Commander
Army Tank Automotive Research & Development Command
ATTN: DRDTA-UL, Library
Warren, MI 48090

Commandant
US Army Aviation Center
P.O. Box O
ATTN: USAAVNT, Library
Ft. Rucker, AL 36362

Director
Army Material Systems Analysis Activity
ATTN: DRXSY-D, Dr. J. Sperrazza
Aberdeen Proving Ground, MD 21005

Commander
Army Communications Research & Development Command
ATTN: DRDCO-SGS
Ft. Monmouth, NJ 07703

Commander
Army Electronics Research & Development Command
Technical Support Activity
ATTN: DELSD-L
Ft. Monmouth, NJ 07703

Commander
Harry Diamond Laboratory
2800 Powder Mill Rd.
ATTN: DELHD-PP, Mr. B. Fonoroff
Adelphi, MD 20783

Commander
US Army Aviation Research & Development Command
P.O. Box 209
ATTN: DRDAV-EVW, Mr. B. Stein
St. Louis, MO 63166

Program Manager
Fighting Vehicle Systems
MAMP Bldg. 1
ATTN: DRCPM-FVS-SEA, Mr. D. Jacobs
Warren, MI 48090

Project Manager, Advanced Attack Helicopter
Product Manager for 30 MM Ammunition
ATTN: DRCPM-AAH-30mm, LTC(P) D. DeLany
Dover, NJ 07801

Project Manager, DIVAD Gun
ATTN: DRCPM-ADG, COL L. Marrella
Dover, NJ 07801

Project Manager, Advanced Attack Helicopter
P.O. Box 209
ATTN: DRCPM-AAH
St. Louis, MO 63166

Commander
US Army Armaments Readiness Command
ATTN: DRSAR-LE, Mr. Artioli
DRSAR-LEI, Mr. Craighead
DRSAR-LED, Mr. Kotecki
DRSAR-LEA, Mr. White
DRSAR-LEP-L, Technical Library
Rock Island, IL 61299

Headquarters
US Army Research & Technical Laboratory
Ames Research Center
ATTN: DAVDL-AS, Mr. W. Andre
Moffett Field, CA 94035

Commander
Watervliet Arsenal
Benet Laboratory
ATTN: Technical Library
Watervliet, NY 12189

Commander
Army Armaments Research & Development Command
ATTN: DRDAR-BL-TD, Dr. Puckett
Aberdeen Proving Ground, MD 21005

Commander
Army Armaments Research & Development Command
ATTN: DRDAR-ACW, Mr. A. Flatau
Aberdeen Proving Ground, MD 21010

Commander (Code 3176)
Naval Weapons Center
ATTN: Mr. P. Miller
China Lake, CA 93555

Commander (Code 50211)
Naval Ordnance Station
ATTN: Mr. N. H. Wood
Louisville, KY 40219

Department of the Navy (Code 5323D)
Naval Air Systems Command
ATTN: Mr. L. Young
Washington, DC 20361

Commander (Code G22)
Naval Surface Weapons Center
ATTN: Mr. C. Samuels
Dahlgren, VA 22448

Commander
Air Force Armament Laboratory
ATTN: ADTC-SD-20, CPT Weinstock
AFATL-DLDG, Mr. Cox
AFATL-DLD, Mr. Mirshak
AFATL-DLDA, Mr. Jenus
AFATL-DLD, Mr. Davis
AFATL-DLDL, Mr. Heiney
Eglin Air Force Base, FL 32548

Deputy for A-10
ATTN: ASD-YXA, MAJ R. Hackford
Wright Patterson, OH 45433

Commanding Officer, Ft. Dix
Armaments Research & Development Command Test Site
Brindle Lake
ATTN: Mr. R. Cooper
Ft. Dix, NJ 08640

Commander
Army Armaments Research & Development Command
ATTN: DRDAR-LC, COL Whalen
DRDAR-SE, COL H. Chesbro
DRDAR-SC, LTC(P) A. Larkins
DRDAR-AC, LTC F. Hackley
DRDAR-SCA-CA, Mr. W. Squire (25)
Dover, NJ 07801

Commander
ARRADCOM
ATTN: DRDAR-TSS (5)
Dover, NJ 07801

Villanova University
Department of Mechanical Engineering
ATTN: Dr. E. V. McAssey, Jr. (6)
Villanova, PA 19085

Director
US Army TRADOC Systems Analysis Activity
ATTN: ATAA-SL (Tech Library)
White Sands Missile Range, NM 88002

Technical Library
ATTN: DRDAR-CLJ-L
Aberdeen Proving Ground, MD 21005

Technical Library
ATTN: DRDAR-TSB-S
Aberdeen Proving Ground, MD 21010

Technical Library
ATTN: DRDAR-LCB-TL
Benet Weapons Laboratory
Watervliet, NY 12189

US Army Materiel Systems Analysis Activity
ATTN: DRXSY-MP
Aberdeen Proving Ground, MD 21005